AN INITIAL INVESTIGATION INTO METHODS OF COMPUTING TRANSONIC AERODYNAMICS SENSITIVITY COEFFICIENTS

AEROSPACE ENGINEERING DEPARTMENT

Semi-Annual Progress Report
July 1, 1987 - December 31, 1987

TEXAS A&M UNIVERSITY

TAMRF Report No. 5802-88-01
February 1988

NASA Grant No. NAG 1-793

Leland A. Carlson
Professor of Aerospace Engineering
Texas A&M University
College Station, Texas 77843-3141

TEXAS ENGINEERING EXPERIMENT STATION

AN INITIAL INVESTIGATION INTO METHODS OF COMPUTING TRANSONIC AERODYNAMIC SENSITIVITY COEFFICIENTS

Semiannual Progress Report

July 1, 1987 -- December 31, 1987

TAMRF Report No. 5802-88-01

February 1988

NASA Grant No. NAG 1-793

Leland A. Carlson
Professor of Aerospace Engineering
Texas A&M University
College Station, TX 77843-3141

AN INITIAL INVESTIGATION INTO METHODS OF COMPUTING TRANSONIC AERODYNAMIC SENSITIVITY COEFFICIENTS

I. Introduction

This report covers the period from July 1, 1987 thru December 31, 1987. The primary tasks during this period were to develop and test methods for computing aerodynamic sensitivity coefficients using the quasi-analytical approach.

II. Personnel

The staff associated with this project during the present reporting period were Dr. Leland A. Carlson, Principal Investigator, and Hesham El Banna, Graduate Research Assistant. It should be noted that the first phase of this research effort has formed the basis for the Masters Thesis research of Mr. El Banna. It is anticipated that Mr. El Banna will receive his M.S. degree in Aerospace Engineering in either May or August 1988.

III. Research Progress

Objectives

Based upon the program outlined in the modified proposal, the initial effort has concentrated on developing the quasi-analytical approach for determining aerodynamic influence coefficients (Ref. 1). In addition, in order to keep these initial efforts computationally efficient and straightforward, it was decided to first consider only two-dimensional flow and to model the problem using the transonic small perturbation equation with surface boundary conditions applied along the slit. The small perturbation equation was selected instead of the full potential equation because it permits the capturing of important nonlinear physical phenomena while being by comparison easy to handle from a coding standpoint. Consequently, the initial objectives have been:

(1) Investigate the feasibility of using the quasi-analytical approach for determining aerodynamic sensitivity coefficients in the transonic regime.

(2) Determine the accuracy of the quasi-analytical approach by comparing results to those computed using finite difference techniques.

(3) Investigate efficient methods for solving the large set of equations associated with the quasi-analytical appraoch.

Problem Statement

Under the quasi-anlytical method, the aerodynamic sensitivity coefficients can be obtained by solving the set of equations

$$\left[\frac{\partial R}{\partial \varphi}\right]\left\{\frac{\partial \varphi}{\partial XD}\right\} = -\left\{\frac{\partial R}{\partial XD}\right\} \qquad (1)$$

where R is the residual expression from the transonic small perturbation equation. I.E.

$$R = (C1 + C2\,\phi_x)\phi_{xx} + \phi_{yy} \qquad (2)$$

$$C1 = 1 - M_\infty * M_\infty \qquad C2 = -(\gamma + 1)\,M_\infty^2$$

In Eq. (1), for a general NxM grid, the system is N*NxM*M; and XD is the design variable of interest. The actual coefficients in Eq. (1) are obtained by evaluating the appropriate analytical expressions using a flowfield solution obtained from Eq. (2) for a given set of conditions. For the present studies, it was decided to limit consideration to two families of airfoils, namely NACA four digit sections and parabolic arc sections whose surface slopes are described by

$$y'_{u,l} = 2C(L-x)/LL \pm 2T(1-2x) \qquad (3)$$

where C= maximum camber, L= chordwise position of maximum camber, T= maximum thickness, and

$$LL = \begin{cases} L*L & \text{for } x <= L \\ (1-L)(1-L) & \text{for } x > L \end{cases} \qquad (4)$$

Consequently, in the surface boundary condition

$$\frac{dy}{dx} = y'_{u,l} - \alpha \qquad (5)$$

there appear the design variables T, α , C, and L. A fifth design variable obviously is the freestream Mach number which enters the problem through the governing differential equation. Thus, in the present studies the design variables considered were

$$XD = \{T, M_\infty, \alpha, C, L\}$$

Now in setting up the complete quasi-analytical problem the circulation and its dependence upon trailing edge potentials must be carefully included. Since the circulation is determined by the difference in potentials at the trailing edge

$$\Gamma = \phi_{u_{TE}} - \phi_{L_{TE}} \qquad (6)$$

and since a branch cut extends from the trailing edge to downstream infinity, the trailing edge potentials appear in the residual expressions for points along the branch cut. In addition, since in the two dimensional case the infinity boundary conditions are proportional to the circulation, the trailing edge potentials also appear in the residual expressions at points adjacent to the outer boundaries. Consequently, the resultant $[\partial R/\partial \phi]$ matrix, while banded, also contains many nonzero elements far from the central band. Obviously, the presence of these elements greatly complicates the rapid and efficient solution of the sensitivty equation, Eq. (1).

Solvers

Flowfield solutions for the present studies were obtained by solving Eq. (2) using an approximate factorization technique similar to that presented in Ref. 2. This approach is considerably more efficient that standard SLOR schemes. In most cases, a 41x20 stretched Cartesian grid based upon a hyperbolic tangent transformation that places the outer boundaries at infinity was utilized, although work is currently in progress with more refined grids. In addition, for these initial studies, the flowfield was normally computed using double precision arithmetic and the maximum residual reduced eight orders of magnitude. It was felt that this level of convergence was necessary in order to accurately evaluate sensitivity coefficients using a finite difference approach, although such convergence may not be required in the flowfield solver for the quasi-analytical method.

Since the primary objective of these initial efforts was to establish the feasibility of the quasi-analytical methods, it was obvious that a reasonably efficient scheme for solving Eq. (1) for the perturbation potential sensitivity coefficients was needed and that an elimination technique, while straightforward, would be too time consuming for such a large system. Consequently, the initial results presented here have been obtained using a Gauss-Seidel iterative scheme. This scheme has not yet been optimized but it does use a sparse matrix approach in that only nonzero elements are stored; and it is considerably faster than elimination approaches. In most cases the error tolerances on the coefficients involving maximum thickness, freestream Mach number and location of maximum camber were 1E-06 while those on angle of attack and maximum camber were 1E-04. Whether or not these can be relaxed in order to permit more rapid solutions is under investigation. In addition, other schemes, such as iterative tridiagonal approaches, are also currently being investigated.

These two solution methods have been combined into a FORTRAN computer program which is menu driven and which can be operated on either microcomputers, small mainframes, or mainframe machines.

Discussion of Initial Results

In these initial studies, the quasi-analytical method has been used to determine aerodynamic sensitivity coefficients at four freestream Mach numbers for two arbitrarily selected airfoils, each at one degree angle of attack. The first is a cambered parabolic arc section having 1% camber at 40% chord, a maximum thickness of 6% at 50% chord, and which is designated P1406; and the second is a NACA 1406 airfoil. In the sections which follow, two types of results will be presented. The first will be plots of $\partial Cpu/\partial XD$ and $\partial Cpl/\partial XD$ versus chord while the second will be $\partial(Cpl-Cpu)/\partial XD$, designated as $\partial\Delta Cp/\partial XD$. In addition, several of the figures will also contain results obtained using the finite difference approach in which each design variable was individually perturbed a small amount, typically 0.001, and a new flowfield solution obtained. Then sensitivity coefficients were computed using $\Delta Cp/\Delta XD$. Finally, tables containing lift coefficient sensitivity coefficient values are presented and will be discussed.

Subsonic Cases, Minf = 0.2

P1406 Airfoil

Initial studies concentrated on subsonic cases since such cases should run quickly and since at least approximate results would be known from thin airfoil theory. Figures 1(a) and 1(b) show the sensitivity of the pressure to thickness for the P1406 airfoil. As expected from thin airfoil theory, the upper and lower surface values are essentially identical and the difference, shown on Fig. 1(b), is very small everywhere. Also, shown on Fig. 1(b) (and on most subsequent figures) by the dashed line is the result obtained using the finite difference approach; and, as can be seen, the agreement between the two approaches is excellent.

The sensitivity of the pressure coefficients to angle of attack are shown for this case on Figures 2(a) and (b). As expected from linear thin airfoil theory, the upper and lower surface curves are essentially equal in magnitude but of opposite sign. Not surprisingly, the sensitivity of the delta Cp variation, Fig. 2(b), has the shape of the pressure difference curve for a flat plate at angle of attack; and its magnitude, particularly near the leading edge is quite large.

On Figures 3(a) and 3(b) is plotted the sensitvity of the pressure coefficient to the amount of maximum camber. Since camber contributes to lift, it is expected from thin airfoil theory that these values should be "equal but opposite in sign" for the upper and lower surfaces. In addition, the pressure difference curve has the correct shape for that associated with a 14 mean line with the peak occuring at 30% chord (Ref. 3) and has magnitudes comparable to those for the $\partial Cp/\partial$ curves.

The sensitivity of pressure to the location of the maximum camber point is portrayed on Fig. 4(a) and (b), and to say the least the results are interesting. Since maximum camber location affects the camber profile and hence lift, the equal and opposite behavior of the upper and lower surface coefficients is expected. In addition, the pressure difference sensitivity is primarily negative forward of the point of maximum camber and positive aft of it. This result indicates that if the location of maximum camber were moved rearward slightly (i.e. a positive Δ L) that lift would be decreased on the forward portion of the airfoil and increased on the aft portion of the airfoil, which is in agremment with the results presented in Ref. 3.

Finally, the sensitivty of pressure to freestream Mach number is plotted on Figs. 5(a) and (b). It should be noticed that while the profiles for the upper and lower surfaces are similar, they are not equal in magnitude, indicating a nonlinear variation with Mach number as predicted by simple Prandtl-Glauret Theory. However, as indicated by the results on Fig. 5(b), the magnitudes for this subsonic Mach number are very low.

NACA 1406 Airfoil

Figures 6-10 show for the NACA 1406 airfoil the sensitivity of Δ Cp with position for each of the five design variables. Since the NACA 1406 and the parabolic P1406 both have the same camber line and since for this low Mach number and thin airfoils the solutions should essentially be linear, the sensitivity to maximum camber and location of maximum camber should be

essentially identical for the two airfoils. As can be seen by comparing Figs. 3(b) with 8 and 4(b) with 9, the present quasi-analytical method does indeed yield this result. Likewise the sensitivity to angle of attack, Figs. 2(b) and 7, are also identical for the two airfoils. However, the pressure sensitivity to thickness, Fig. 6, and freestream Mach number, Fig. 10, while very small in magnitude compared to the other coefficients, has a different chordwise variation than that for the P1406 airfoil. The first, of course, is expected since the two airfoils have different thickness distributions; and the second is due to the fact that the two airfoils have entirely different pressure distributions and, thus, sensitivity to Mach number.

Once the sensitivities of the potentials and/or Cp distribution to the design variable are known, the sensitivity of the lift coefficients to the design variables can be easily computed. To minimize errors, for these cases these coefficients have been computed using

$$CL = 2* \text{Circulation} = 2*(\Phi_{u_{TE}} - \Phi_{L_{TE}})$$

whence

$$\frac{\partial CL}{\partial XD} = 2\left(\frac{\partial \Phi_{u_{TE}}}{\partial XD} - \frac{\partial \Phi_{L_{TE}}}{\partial XD}\right)$$

and the results are shown on Table I. It should be noticed that for the subsonic case that the lift sensitivites for the two airfoils are essentially identical. Since these airfoils are thin and since they have the same camber line, such agreement should exist.

Transonic Cases -- Minf = 0.8

P1406 Airfoil

For this case, the cambered parabolic airfoil is slightly supercritical with a weak shock on the upper surface at about 55% chord; and the lower surface is entirely subcritical with the minimum pressure point occuring at 60% chord. As a consequence the variation with chord of the sensitivity coefficients is considerably different than in the subsonic case. Figures 11(a) and (b) show the sensitivity of pressure to the maximum thickness; and while the lower surface profile is similar to that obtained at subsonic conditions, the upper surface curve and the pressure difference coefficient plot show the effect of the upper surface shock wave. The large peak on the curves corresponds to the location of the shock wave and indicates that the shock wave location is very sensitive to maximum thickness. Notice on Figures 11(a) and (b) the excellent agreement of the quasi-analytical results indicated by the solid lines with those obtained using the finite difference approach (dashed lines).

The results for $\partial Cp/\alpha$ and $\partial \bar{C}p/\alpha$, which are shown on Figures 12(a) and (b), are similar. The lower surface curve is typical of a subsonic flow, while the upper surface and the pressure difference coefficients reflect the presence of the upper surface shock wave. Similar comments can be made for the remaining design variable coefficients, which are plotted on Figures 13 - 15.

Examination of the curves in the vicinity of the shock wave location indicates that the pressure sensitivity and indirectly shock wave location is about equally influenced by angle of attack, maximum thickness, and freestream Mach number. However, in comparison it is relatively insensitive to location of maximum camber; but, perhaps surprisingly so, the pressure is twice as sensitive to the amount of maximum camber as it is to the other design variables.

NACA 1406

At Minf=0.8, the flow about the NACA 1406 airfoil has a strong shock at 40% chord. As a result the pressure design sensitivity coefficients, which are shown on Figures 16 - 20, have large peaks at the shock location. In addition, while the curves are similar to those obtained for the P1406 airfoil, they differ in details and some cases in magnitudes. In particular, the peak value at the shock in the $\partial Cp/\partial$ curve for the NACA 1406 is significantly higher than that for the P1406 airfoil. Further, for the subsonic "linear" flow situation the sensitivity coefficients for angle of attack, maximum camber and location of maximum camber were identical for the two airfoils. However, at transonic conditions, the flow is highly nonlinear and the corresponding curves for the two airfoils are significantly different. Again the reasonable agreement between the quasi-analytical results (solid lines) and the finite difference results (dashed lines) is evident on the figures.

The sensitivity of lift to the design variables is also shown on Table I for both airfoils. While the values for the various design variables are similar in magnitude for the two airfoils, there are some significant differences. For example, the coefficients for maximum thickness differ by a factor of two between the two airfoils and those for Mach number differ by about fifty percent. Also, it should be noticed that for both airfoils the lift is most sensitive to angle of attack and to maximum camber.

Accuracy of the Quasi-Analytical Method

In order to verify the accuracy of the quasi-analytical method, design sensitivity coefficients for Cp and CL were obtained using the finite difference approach. In this procedure, a single design variable was perturbed by typically 0.001, while all others remained constant, and a new flowfield solution obtained using the approximate factorization solver. Then values of the various sensitivity coefficients were then obtained by finite differences. The results obtained in this manner for the pressure distributions have been shown on the various figures by dashed lines, and in many cases the dashed lines are coincident with the quasi-analytical results (solid lines). In addition, Table II compares results obtained by the two methods at Mach numbers of 0.2, 0.8 and 1.2. In most cases the agreement is significantly less than 1 percent. Similar numbers were also obtained for the Mach 0.825 P1406 case, and there the agreement between the two procedures was not nearly as good. It is believed that of the two sets of values the quasi-analytical results are probably better and that the differences are due to the rapidly changing shock strength etc. occurring around Mach 0.825.

Freestream Mach Number Studies

Transonic Case -- Minf = 0.825, P1406 Airfoil

In an attempt to determine the behavior of the design sensitivity coefficients with Mach number, results were obtained for the P1406 airfoil at a freestream

Mach number of 0.825. At these conditions, the lower surface pressures are still subcritical. However, in contrast to the case at Minf=0.8, the upper surface has for this Mach number a strong shock wave at about 70% chord. Consequently, the aerodynamic sensitivity coefficient curves, which are shown on Figures 21-25, are in the vicinity of the shock wave similar in shape to those for the NACA 1406 at Minf = 0.8, which also had a strong shock wave. In addition, the peaks are larger in magnitude than those at Mach 0.8 and further aft, showing the dependence on shock wave location. However, the lower surface curves are almost unchanged.

Table III compares the lift coefficient sensitivity to the design variables at various freestream Mach numbers for the cambered parabolic airfoil. Comparison of the results at Mach 0.8 and 0.825 shows that $\partial CL/\partial T$ and $\partial CL/\partial M_\infty$ changed significantly between the two Mach numbers. It is believed that the reason for these large changes is that between Mach 0.8 and 0.825, the shock wave on the upper surface is rapidly increasing in strength and the size of the supersonic zone is rapidly growing. However, once the strong shock pressure distribution is established the coefficients drop. In fact, comparison of the P1406 results at Mach 0.825 and the NACA 1406 at Mach 0.8 indicates that these coefficients for the two airfoils are very similar in magnitude. Of course, both cases have strong shock waves on the upper surface.

Supersonic Case, Minf = 1.2, P1406 Airfoil

In order to investigate the applicability of the quasi-analytical method at supersonic freestream Mach numbers, a solution was obtained for the P1406 airfoil at Mach 1.2. At this condition, the flow is transonic in that the bow shock is detached, and there is a region of subsonic flow extending to approximately the quarter chord. Figures 26-30 show the pressure sensitivities for this case, and Table III lists the lift sensitivites. Examination of the plots shows that the pressure sensitivity coefficients have different trends and magnitudes from those computed for subsonic freestream supercritical conditions, Figs. 11-15 and 21-25, and that they are approaching the form expected from supersonic linear theory. These changes are particularly evident in the lift derivatives presented in Table III. Notice that the derivatives with respect to the design variables maximum thickness, Mach number, and location of maximum camber have switched sign. In addition, as expected from linear theory, the influence of camber on lift has decreased significantly; and at M=1.2 is only about 25% of the angle of attack effect as compared to a factor of about two at M=0.8.

Time Comparisons

Obviously, in the development of the quasi-analytical method it is hoped that not only will this approach yield accurate values for the aerodynamic sensitivity coefficients but also that it will be more efficient than the brute force finite difference approach. Table IV presents some comparisons concerning the amount of computational effort required to obtain solutions by the two approaches.

It comparing the values several items should be kept in mind. First, it has been assumed that the finite difference approach will require six independent solutions. In practice it might be possible to start each finite difference solution from a previous solution and, thus, decrease the time to convergence. However, to be accurate, the finite difference approach will probably require

double precision and will have to be extremely well converged (i.e. 1E-08). Nevertheless, the values for the finite difference approach probably should be viewed as maximum values.

Second, the Gauss-Sidel method for obtaining the sensitivity coefficients has not been optimized and may not even be an efficient method; and the flowfield solution required for the quasi-analytical approach may not need double precision and may not have to be as tightly convered. Thus, the values shown for the quasi-analytical approach should also be viewed as maximum values.

In spite of these limitations, the present results do indicate, at least for the present grid of only 41x20, that the quasi-analytical method is at transonic conditions potentially more computationally efficient than the brute force finite difference approach.

IV. Future Efforts

During the next reporting period, work will continue on developing the quasi-analytical approach to computing aerodynamic sensitivity coefficients in the transonic flow regime. In particular, studies will be conducted using more refined grids at variety of freestream Mach numbers. Also, new solution schemes for the quasi-analytical equation, Eq. (1), will be considered and tried. In addition, the concept of only including part of the flowfield in Eq.(1) in attempt to reduce the size of the system will be investigated. This approach may not be practical at subsonic speeds, but may have some applicability at transonic velocities, and definitely can be used at supersonic freestream conditions. It is anticipated that all of these efforts will be restricted entirely to two-dimensional flows.

Finally, it is also anticipated that a proposal will be submitted to continue this work and to extend it to three dimensional transonic flows about wings.

IV. References

1. Sobieski, J. "The Case for Aerodynamic Sensitivity Analysis", Paper presented to NASA/VPI&SY Symposium on Sensitvity Analysis in Engineering, September 25-26, 1986.

2. Ballhaus, W. F., Jameson, A., and Albert, J., "Implicit Approximate Factorization Schemes for Steady Transonic Flow Problems," AIAA Journal, Vol. 16, No. 6, JUne 1978, pp. 573-579.

3. Abbott, I. H. and Von Doenhoff, A. E., Theory of Wing Sections, Dover, New York., 1959.

TABLE I -- Comparison of Lift Sensitivity Coefficients for Similar Parabolic and NACA Airfoils (Quasi-Analytical Method)

Design Variable	Minf = 0.2		Minf = 0.8	
	P1406	NACA 1406	P1406	NACA 1406
Max. Thickness	0.0056	0.0050	1.1171	0.6069
Angle of Attack	6.3529	6.3532	11.0361	10.8541
Max. Camber	10.4638	10.4595	21.4718	19.6335
Loc. of Max. Camber	0.0814	0.0813	0.1843	0.1648
Minf	0.0493	0.0489	1.4381	1.0150

TABLE II -- Accuracy of Quasi-Analytical Method for Computing oCL/oXD Sensitivity Coefficients for P1406 Airfoil

Design Variable	Minf = 0.2		Minf = 0.8		Minf = 1.2	
	Quasi-Analy	Finite Diff	Quasi-Analy	Finite Diff	Quasi-Analy	Finite Diff
Max. Thickness	0.0056	0.0058	1.1171	1.1163	-0.2505	-0.2476
Angle of Attack	6.3529	6.3603	11.0361	11.0508	5.0899	5.0920
Max. Camber	10.4638	10.4710	21.4718	21.5139	1.3152	1.3279
Loc. of Max. Camber	0.0814	0.0818	0.1843	0.1849	-0.1121	-0.1114
Minf	0.0493	0.0495	1.4381	1.4448	-0.1259	-0.1252

TABLE III -- Comparison of Lift Sensitivity Coefficients at Different Freestream Mach Numbers for the P1406 Airfoil (Quasi-Analytical Method)

Design Variable	Freestream Mach Number			
	0.200	0.800	0.825	1.200
Max. Thickness	0.0056	1.1172	0.6524	-0.2505
Angle of Attack	6.3529	11.0361	11.4174	5.0899
Max. Camber	10.4638	21.4718	21.5506	1.3152
Loc. of Max. Camber	0.0814	0.1843	0.1652	-0.1121
Minf	0.0493	1.4381	1.0781	-0.1259

TABLE IV -- Time Comparisons for Obtaining Sensitivity Coefficients for Five Design Variables for the P1406 Airfoil

	Minf = 0.2	Minf = 0.8	Minf=1.2
Flowfield Solver	1	2.95	2.30
Finite Difference Approach (6 Flowfield Solutions)	6	17.70	13.80
Quasi-Analytical Approach (1 Flowfield Solution plus Sensitivity Coefficient Solution via Gauss-Sidel)	4.54	7.45	5.52
Ratio -- QA/FD	0.76	0.42	0.40

Note: All times are normalized by the flowfield solver time at Mach 0.2. Grid 41x20

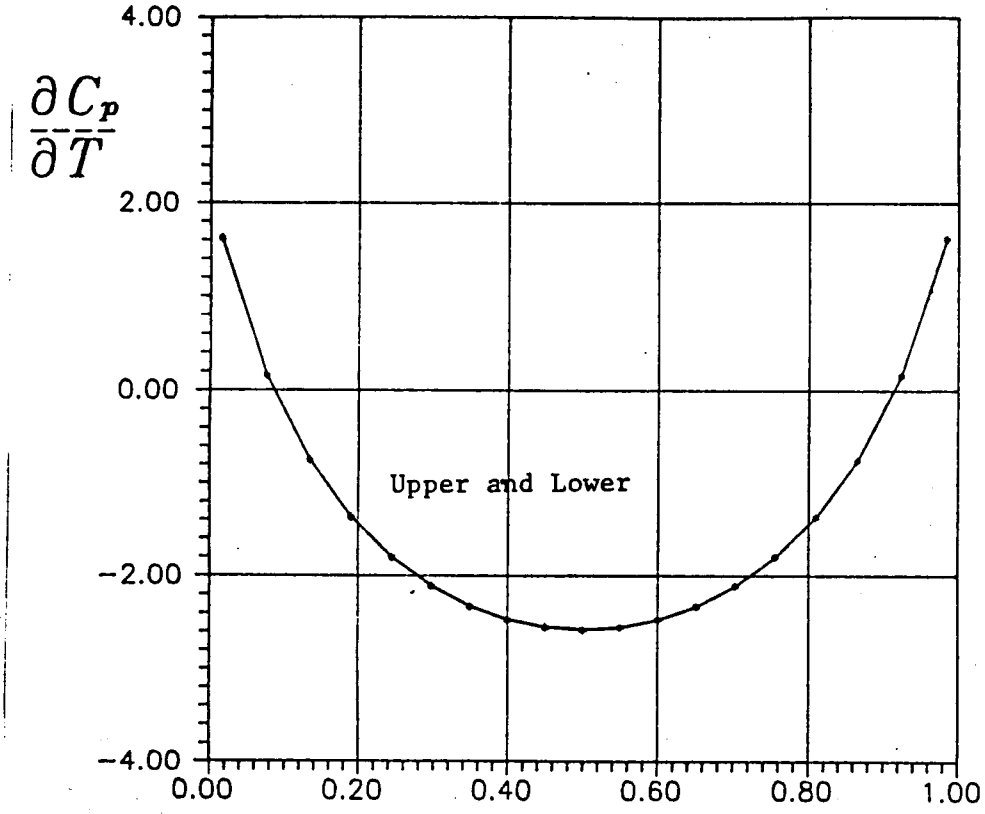

(a)

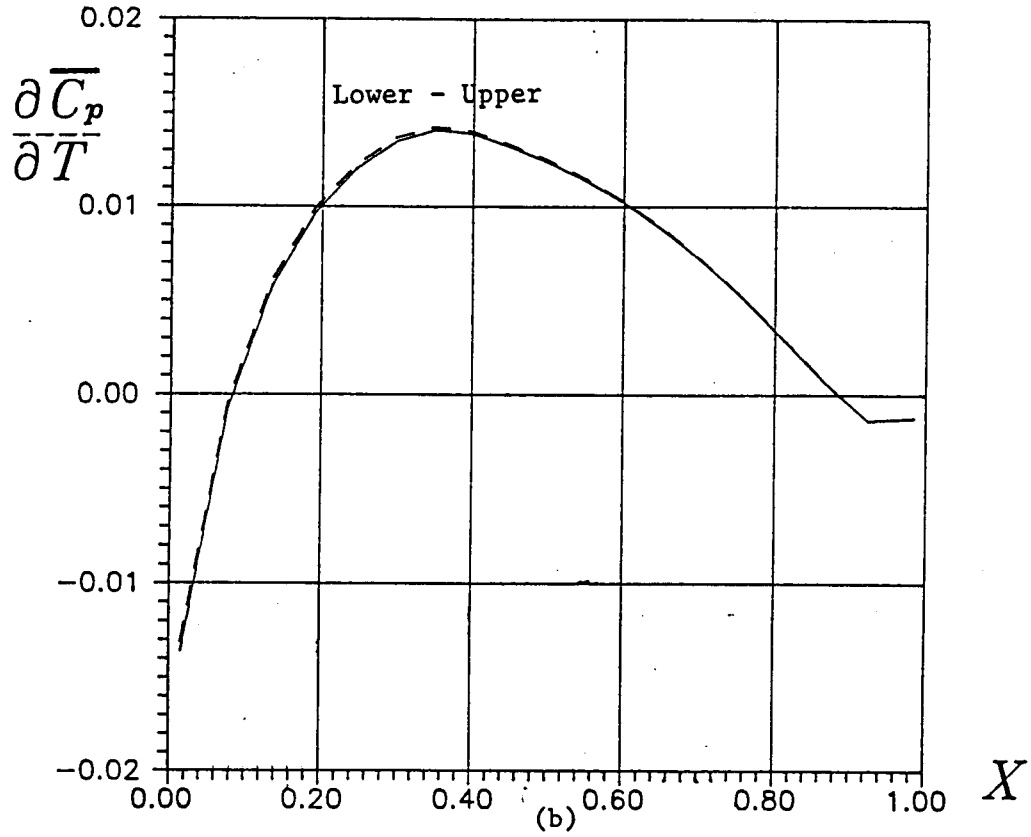

(b)

Figure 1 -- Sensitivity of Pressure to Maximum Thickness

P1406 Airfoil M = 0.2 α = 1 degree

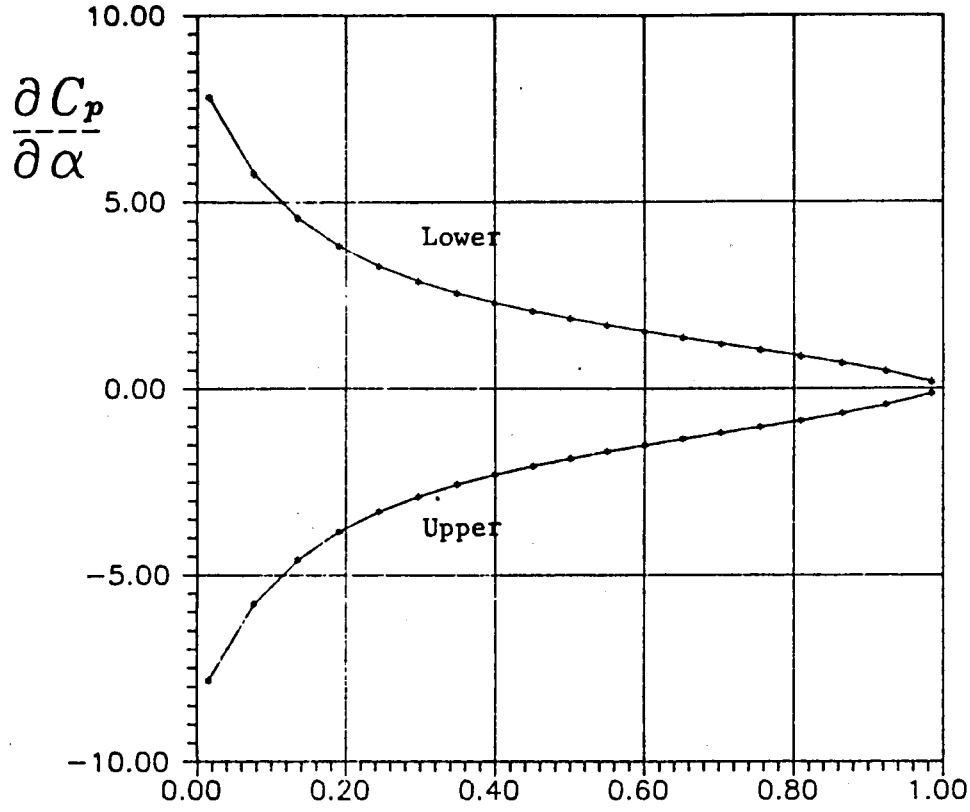

(a)

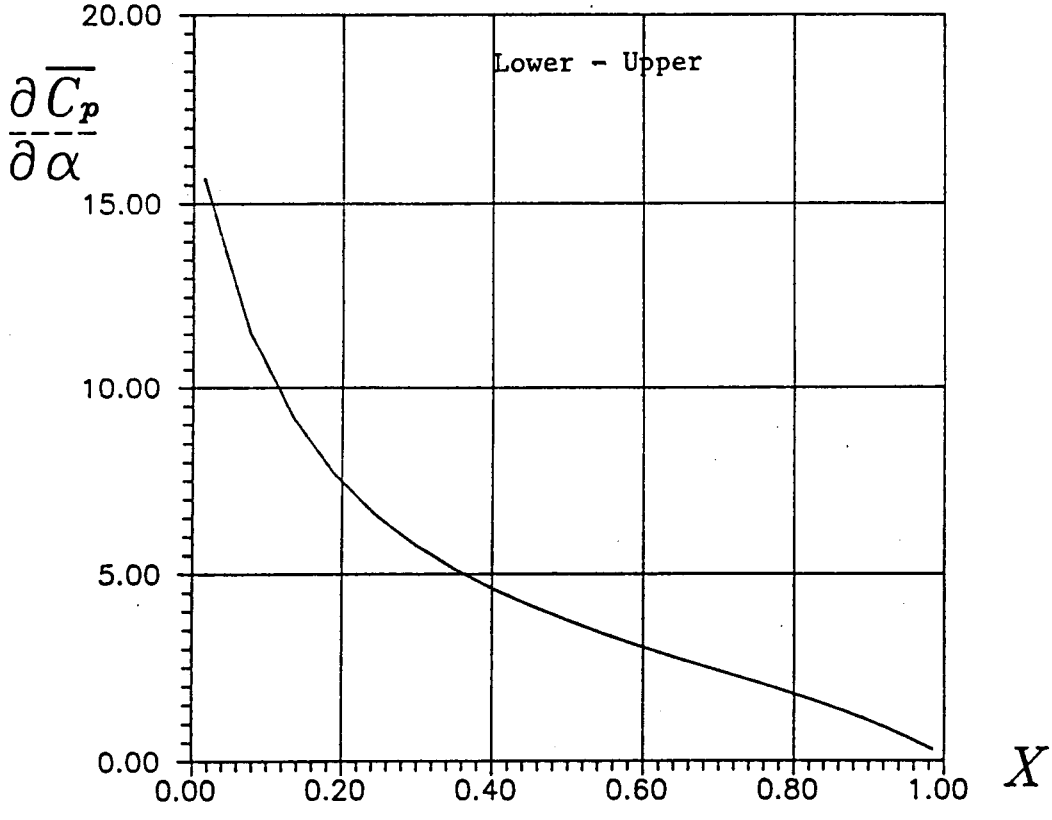

(b)

Figure 2 -- Sensitivity of Pressure to Angle of Attack

P1406 Airfoil M = 0.2 α = 1 degree

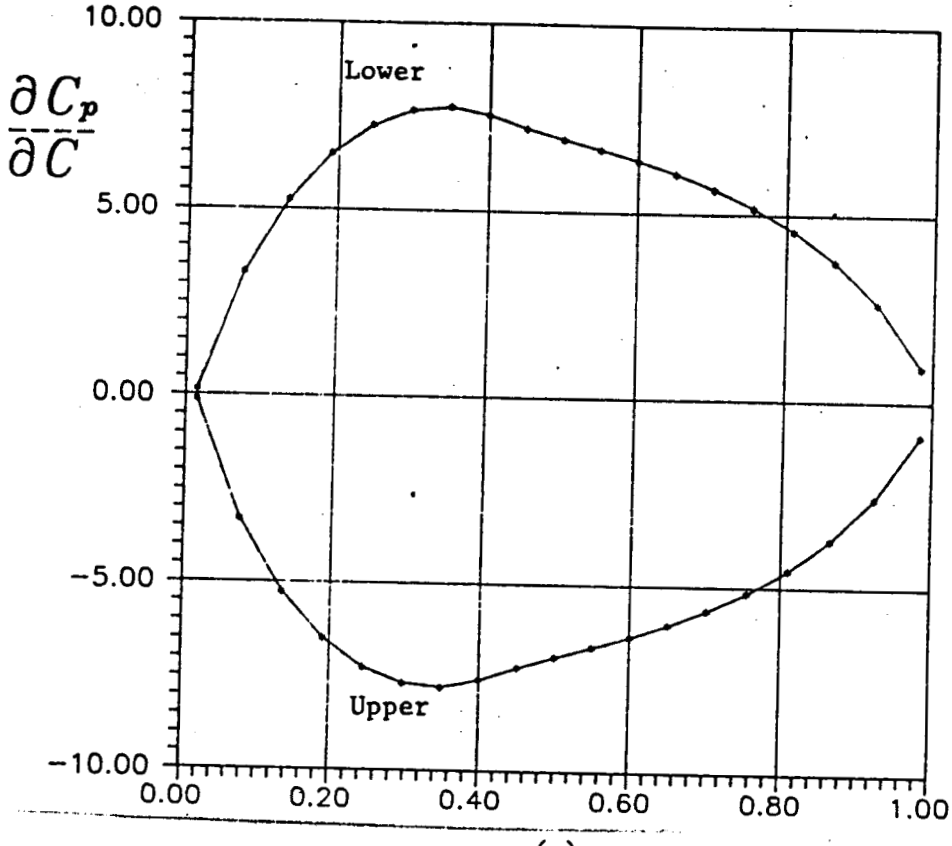

(a)

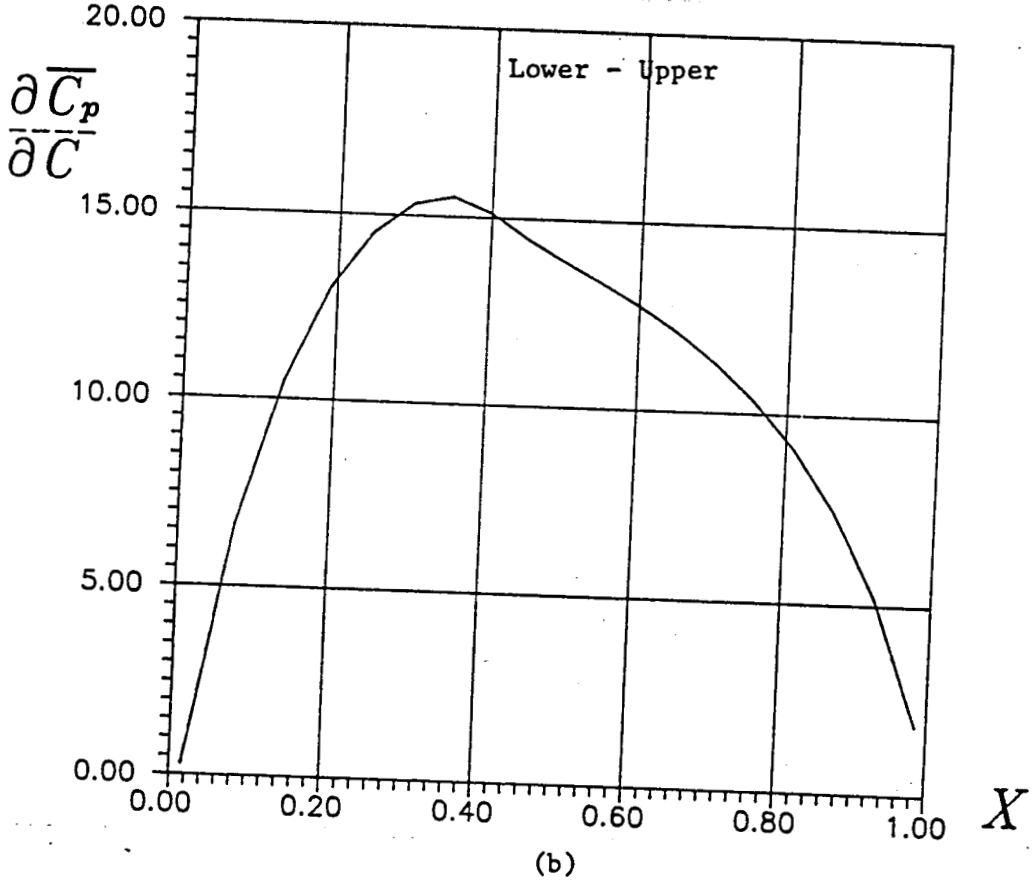

(b)

Figure 3 -- Sensitivity of Pressure to Maximum Camber
P1406 Airfoil M = 0.2 α = 1 degree

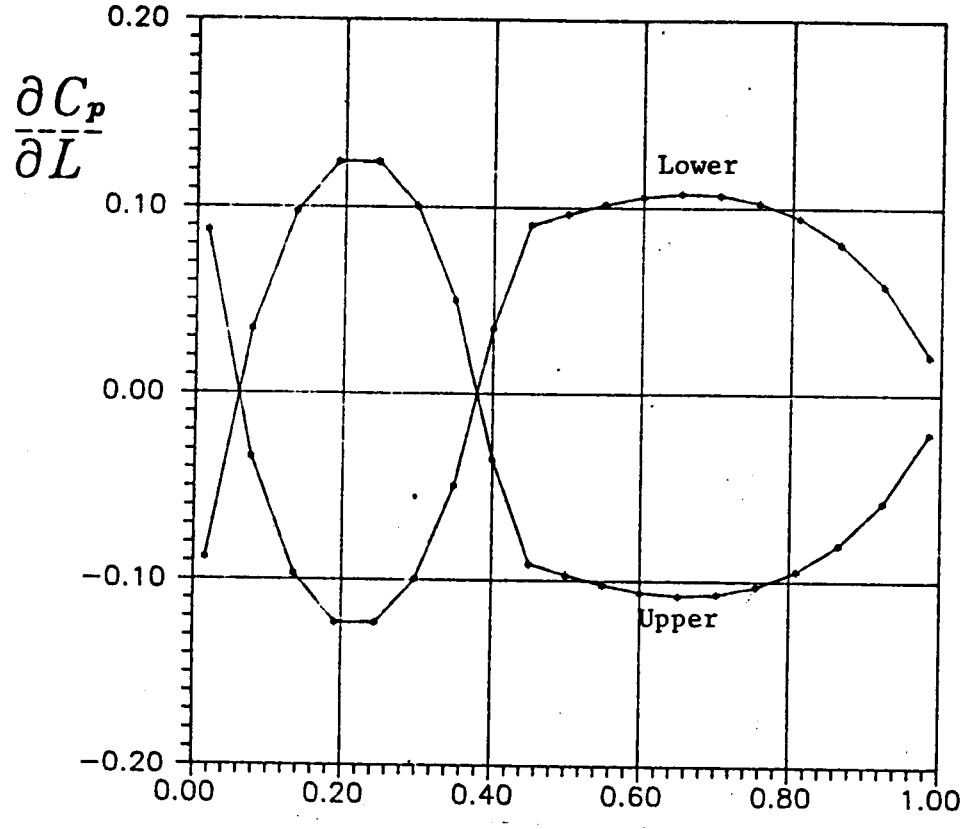

(a)

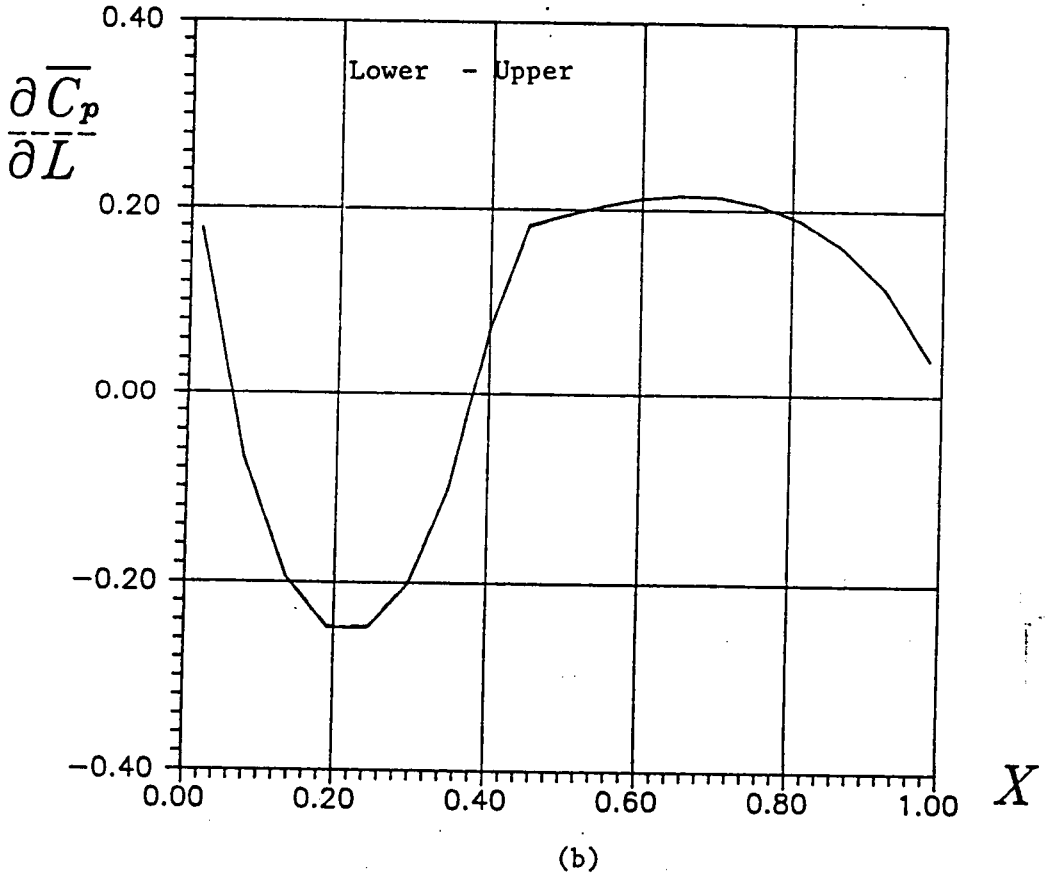

(b)

Figure 4 -- Sensitivity of Pressure to Location of Maximum Camber
P1406 Airfoil M = 0.2 α = 1 degree

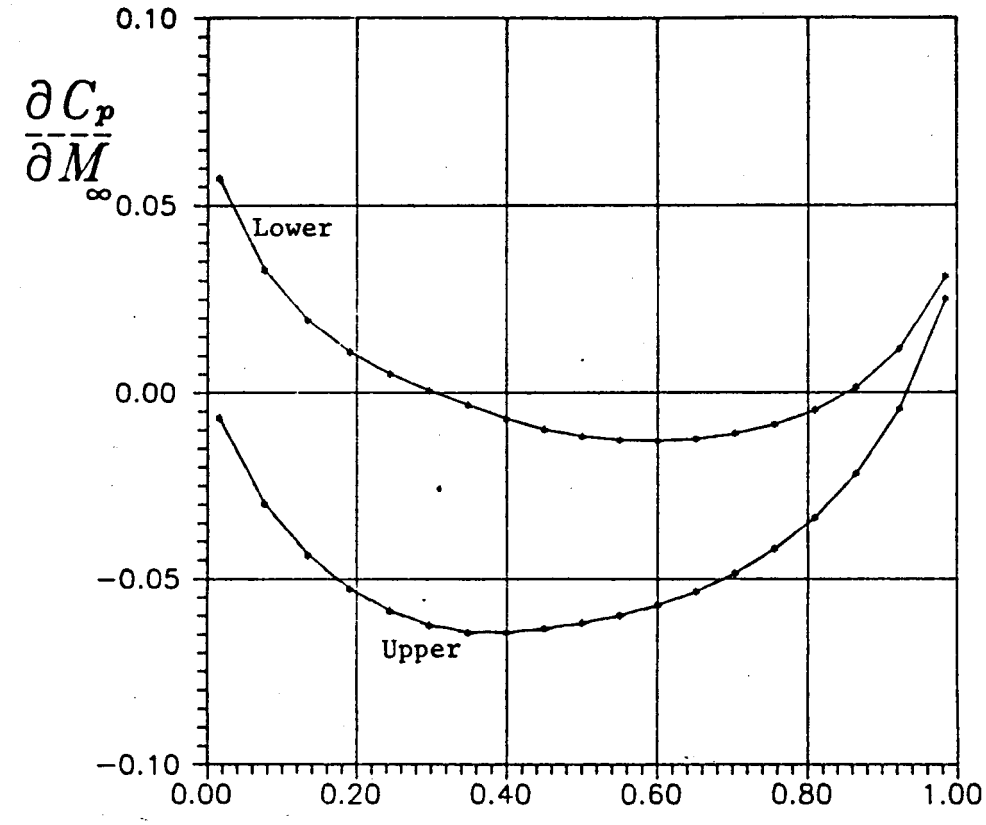

(a)

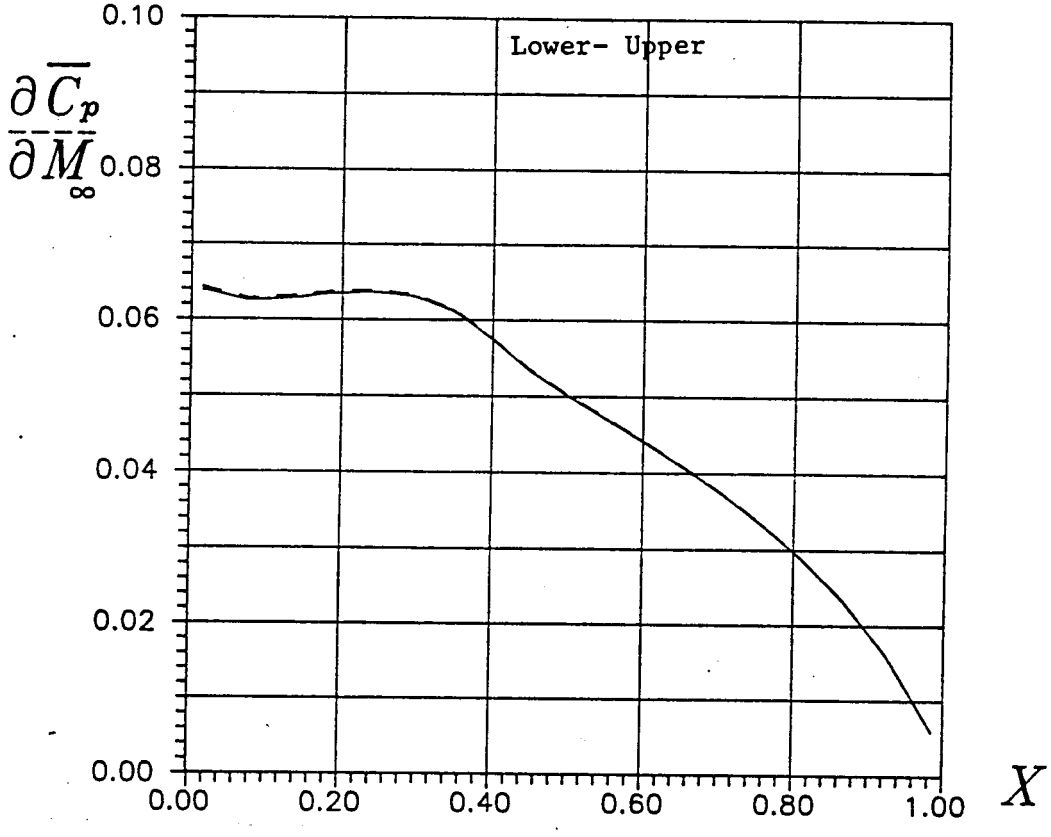

(b)

Figure 5 -- Sensitivity of Pressure to Mach Number
P1406 Airfoil M = 0.2 α = 1 degree

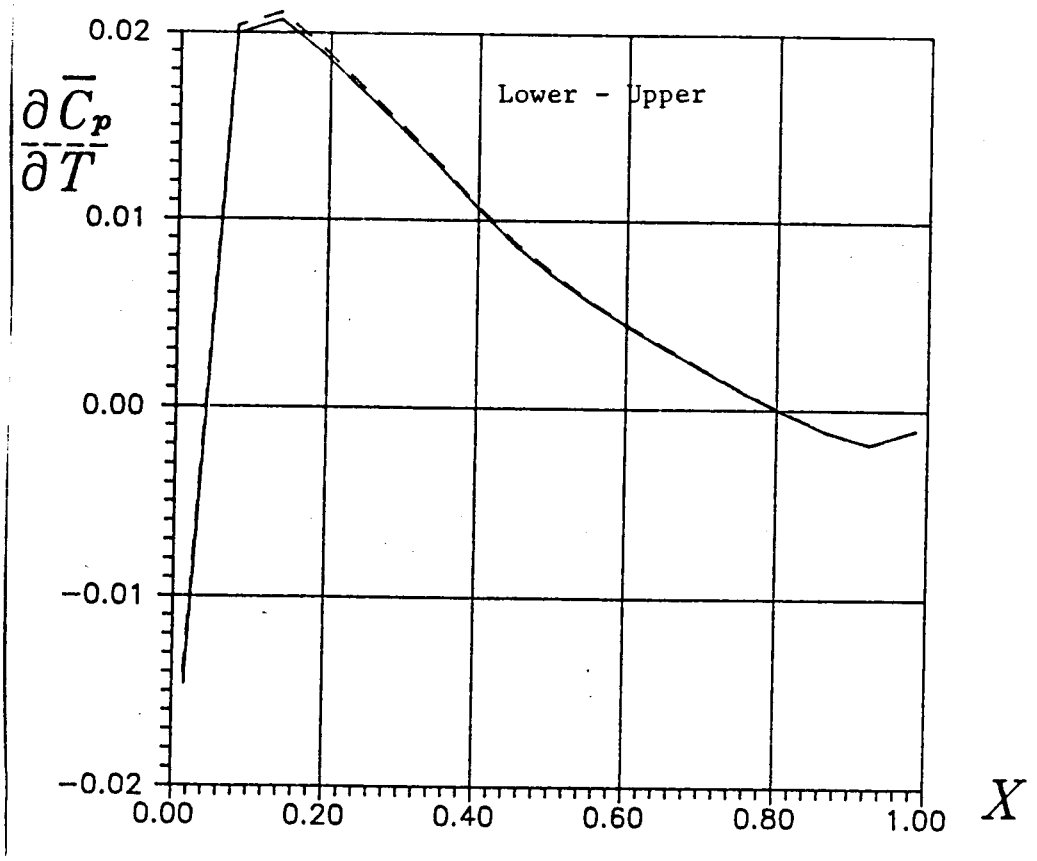

Figure 6 -- Sensitivity of Pressure to Maximum Thickness
NACA 1406 Airfoil M = 0.2 α = 1 degree

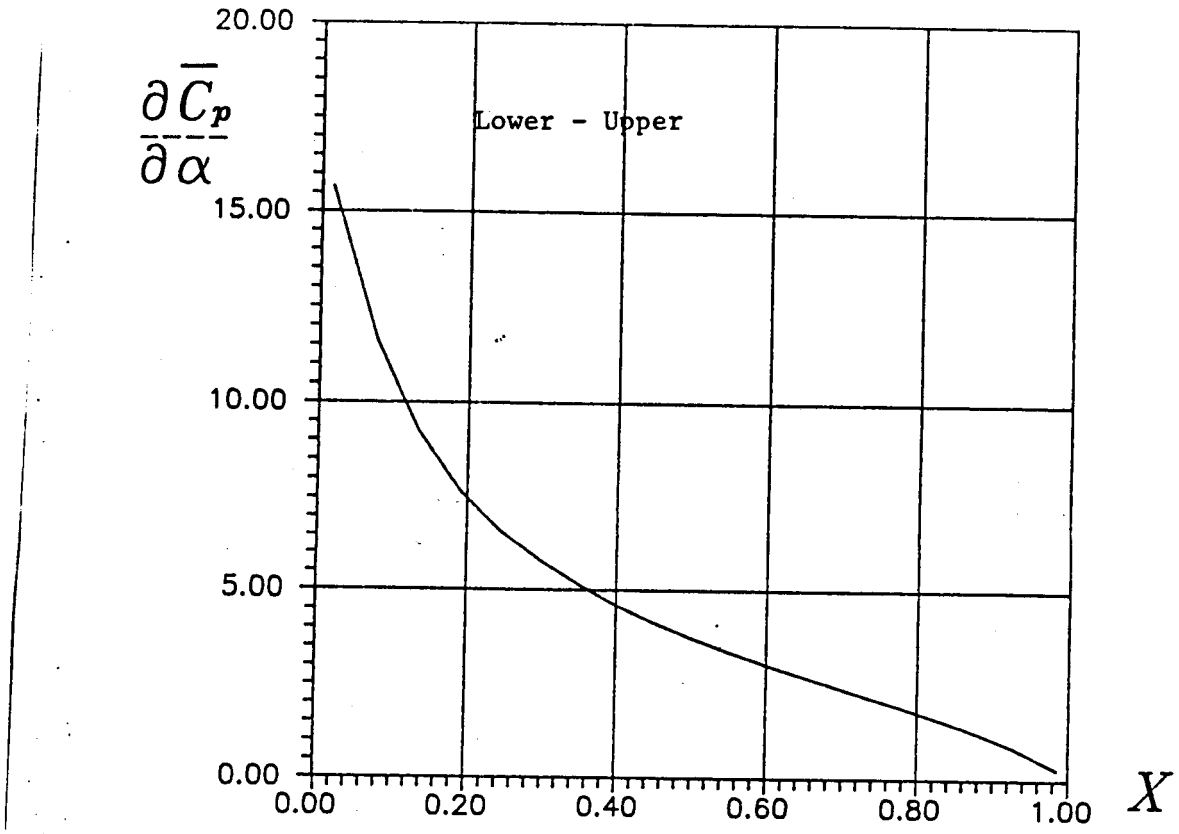

Figure 7 -- Sensitivity of Pressure to Angle of Attack

NACA 1406 Airfoil M = 0.2 α = 1 degree

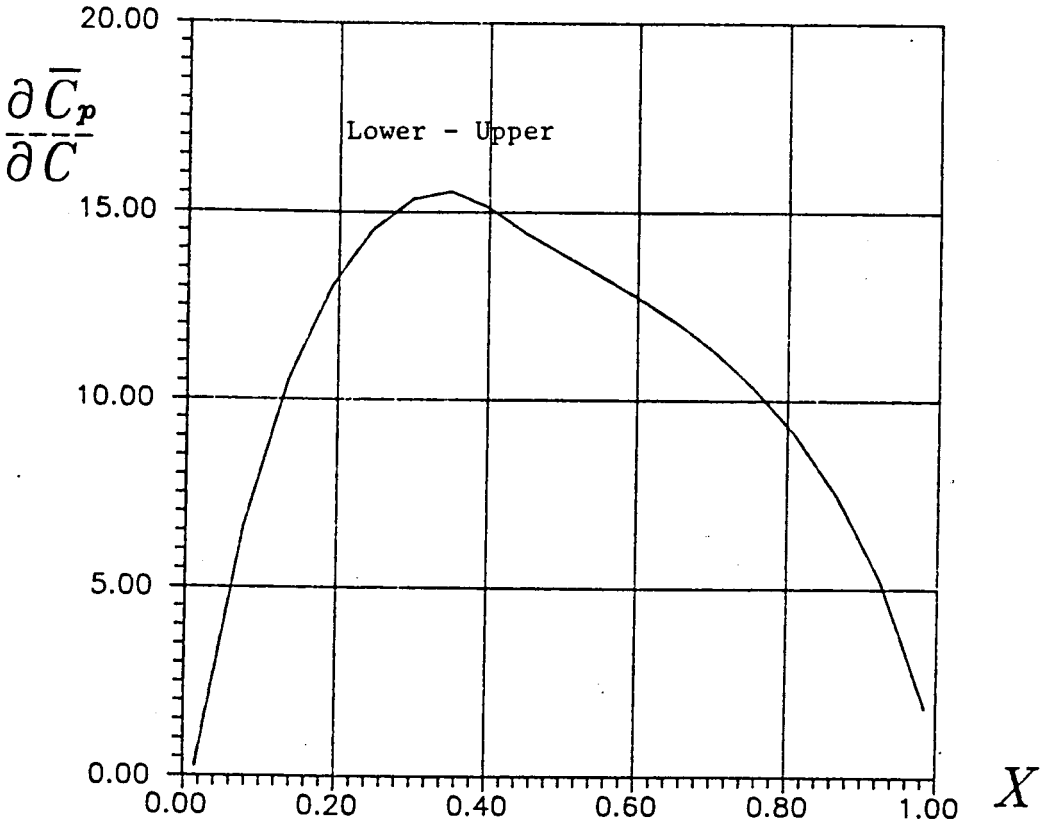

Figure 8 -- Sensitivity of Pressure to Maximum Camber
NACA 1406 Airfoil M = 0.2 α = 1 degree

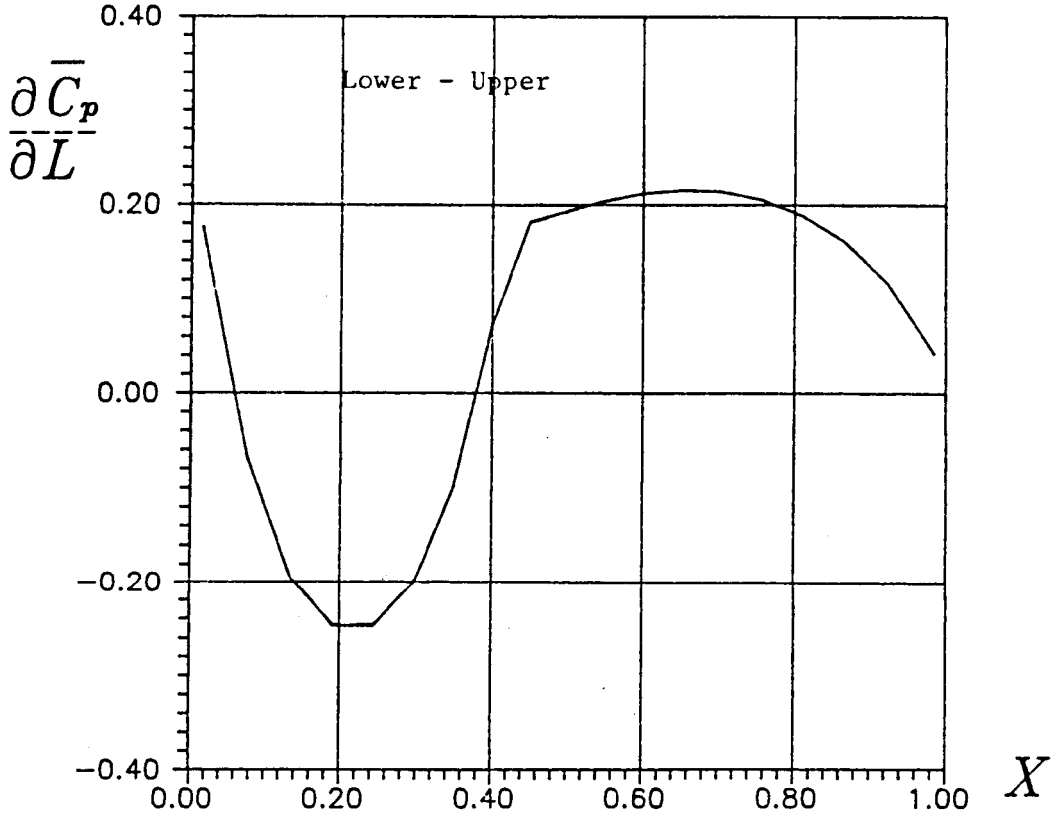

Figure 9 -- Sensitivity of Pressure to Location of Maximum Camber
NACA 1406 Airfoil M = 0.2 α = 1 degree

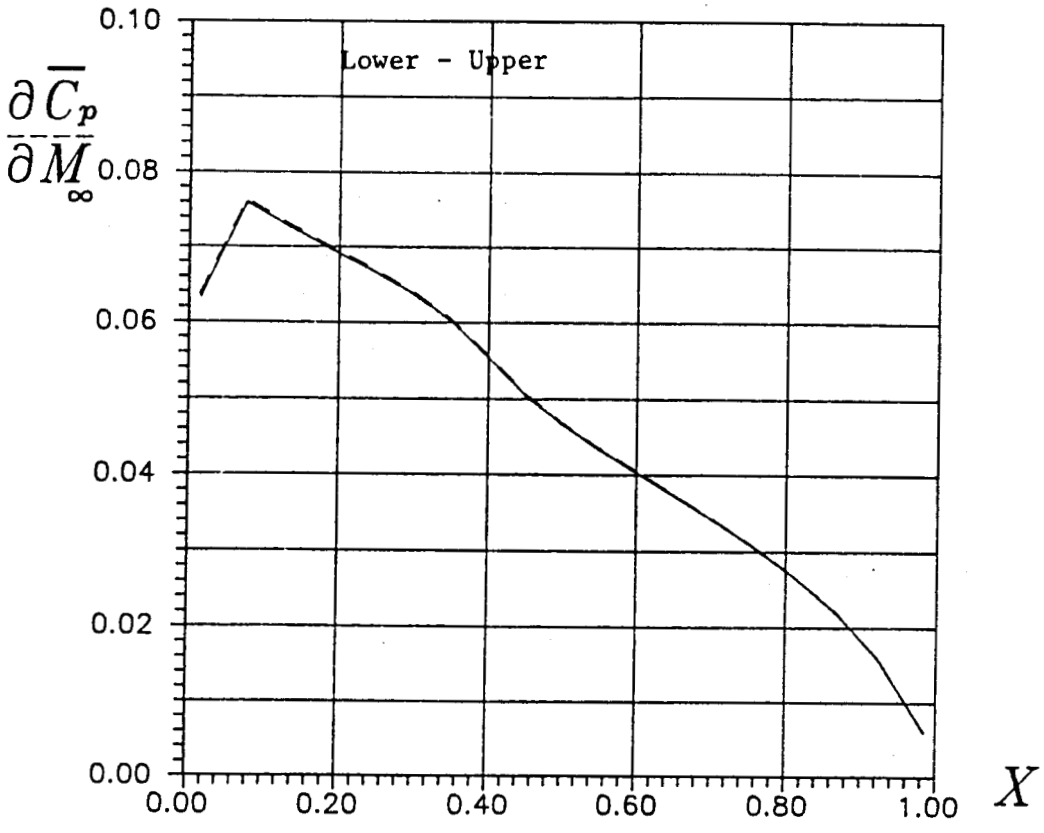

Figure 10 -- Sensitivity of Pressure to Mach Number
NACA 1406 Airfoil M = 0.2 α = 1 degree

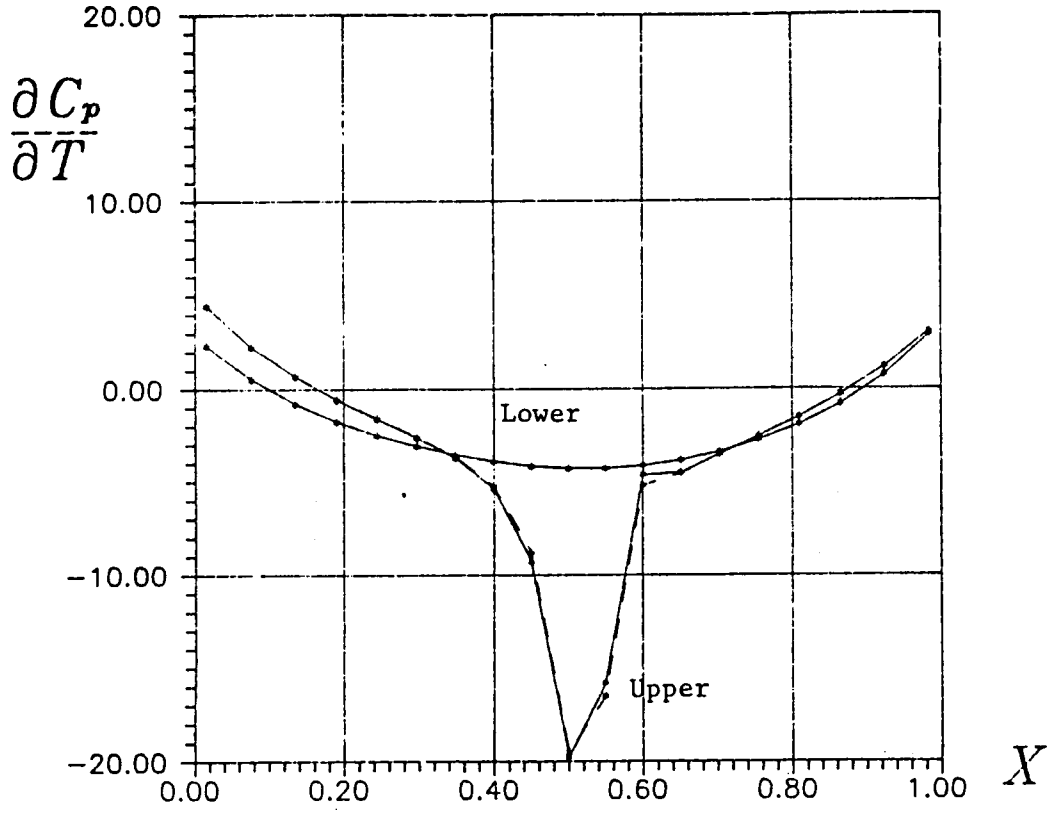

(a)

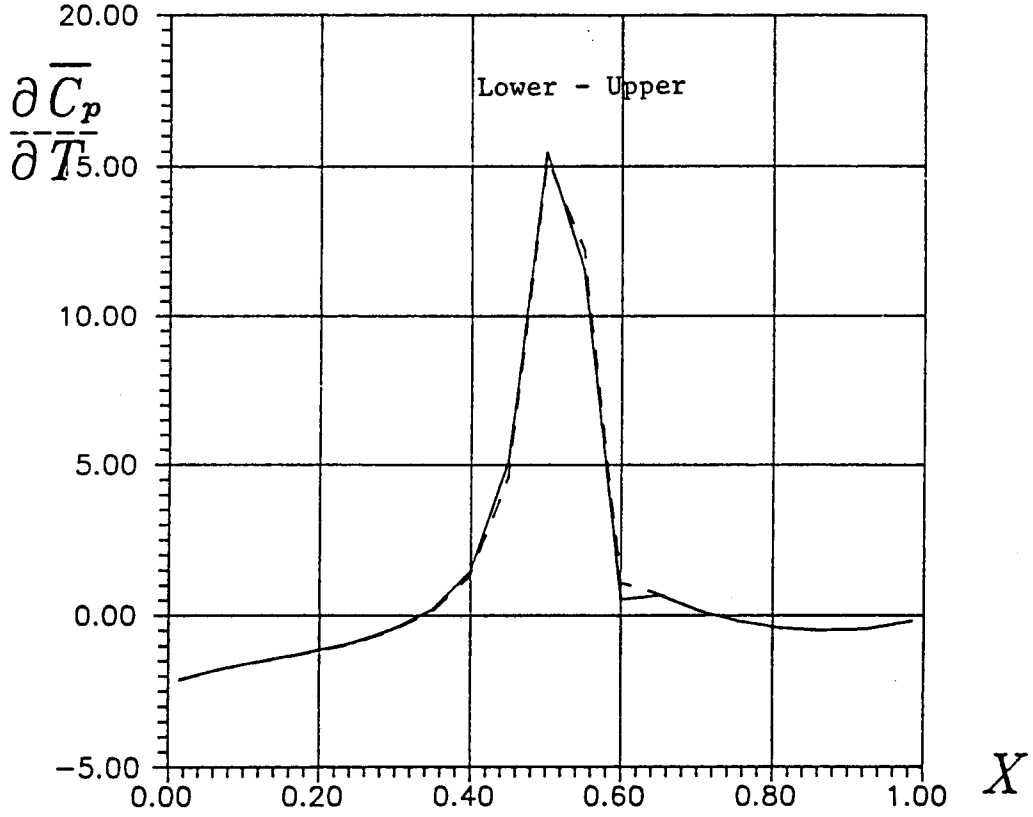

(b)

Figure 11 -- Sensitivity of Pressure to Maximum Thickness
P1406 Airfoil M = 0.8 α = 1 degree

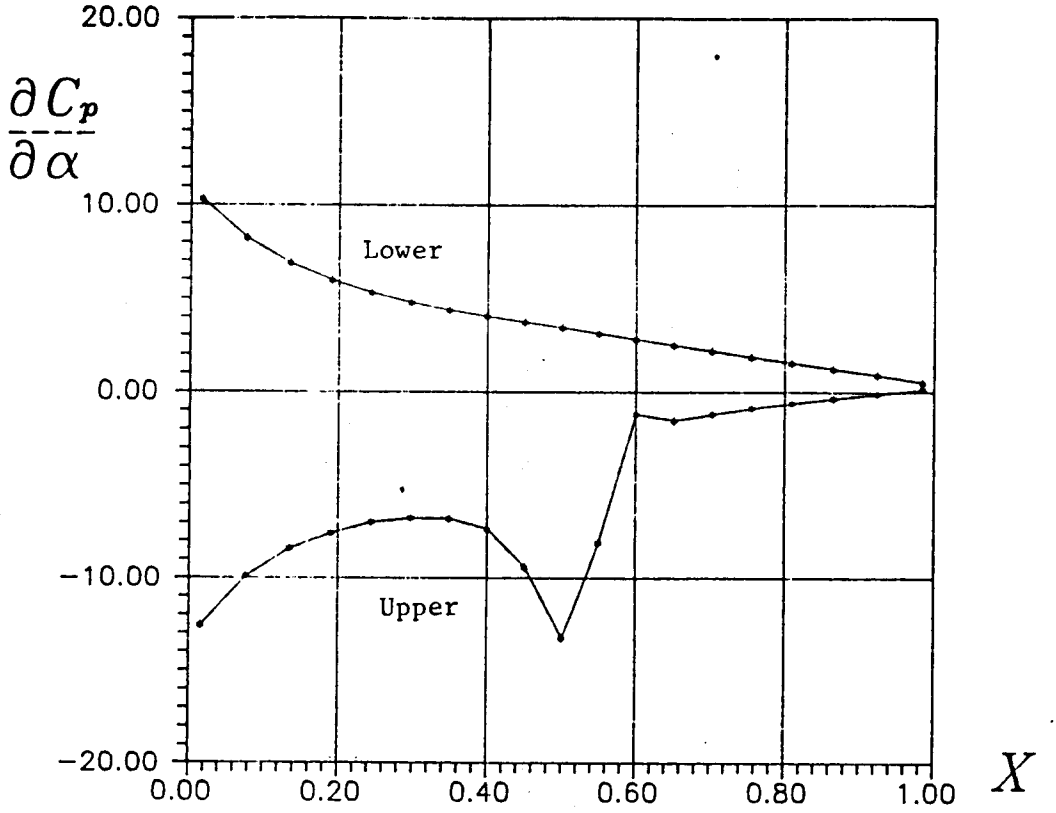

(a)

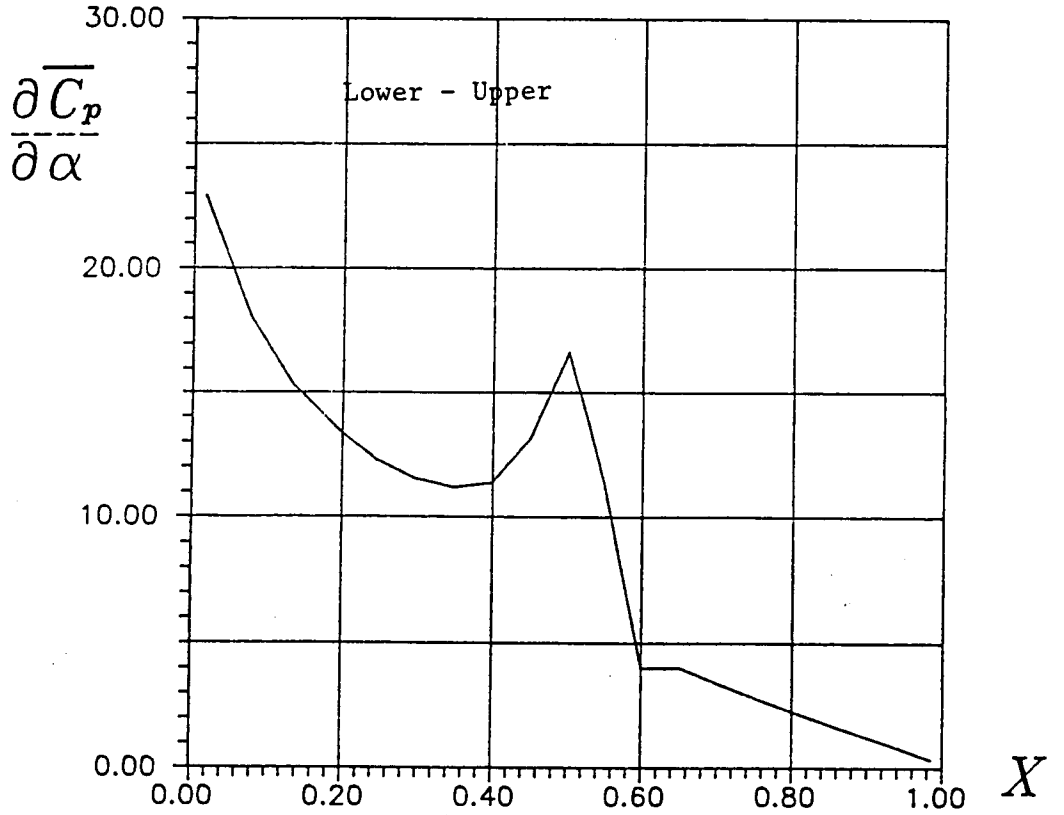

(b)

Figure 12 -- Sensitivity of Pressure to Angle of Attack
P1406 Airfoil M = 0.8 α = 1 degree

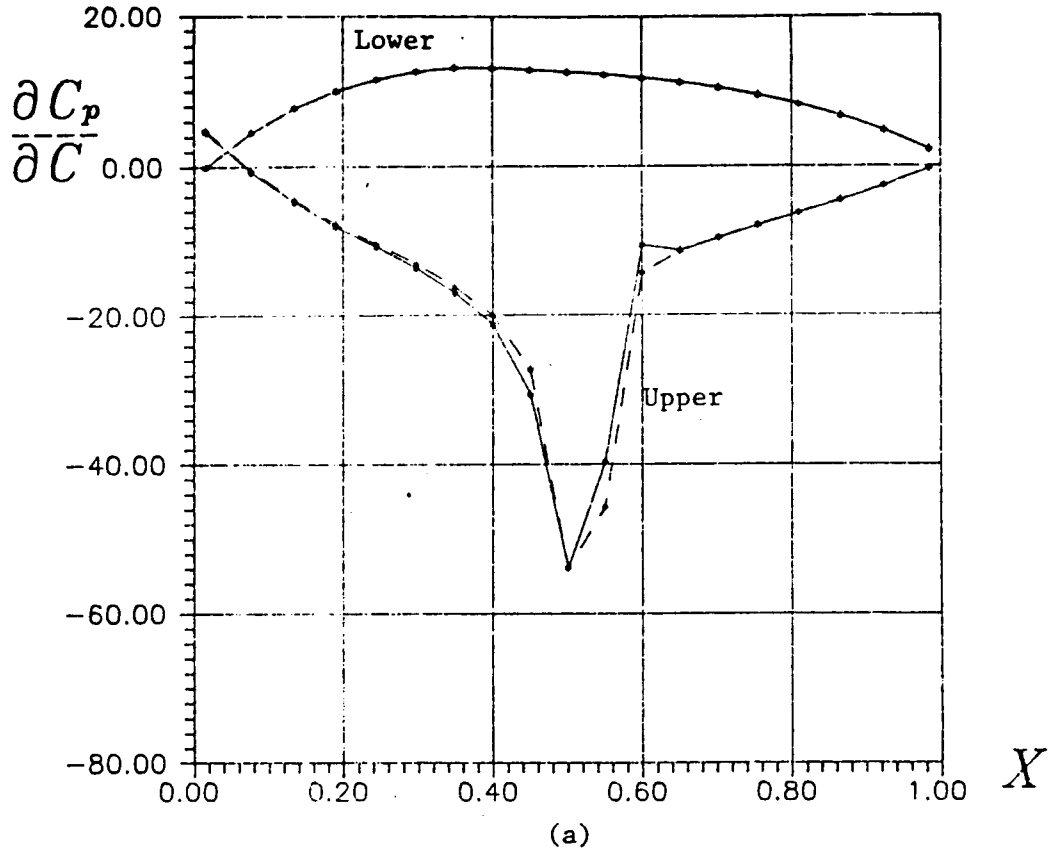

(a)

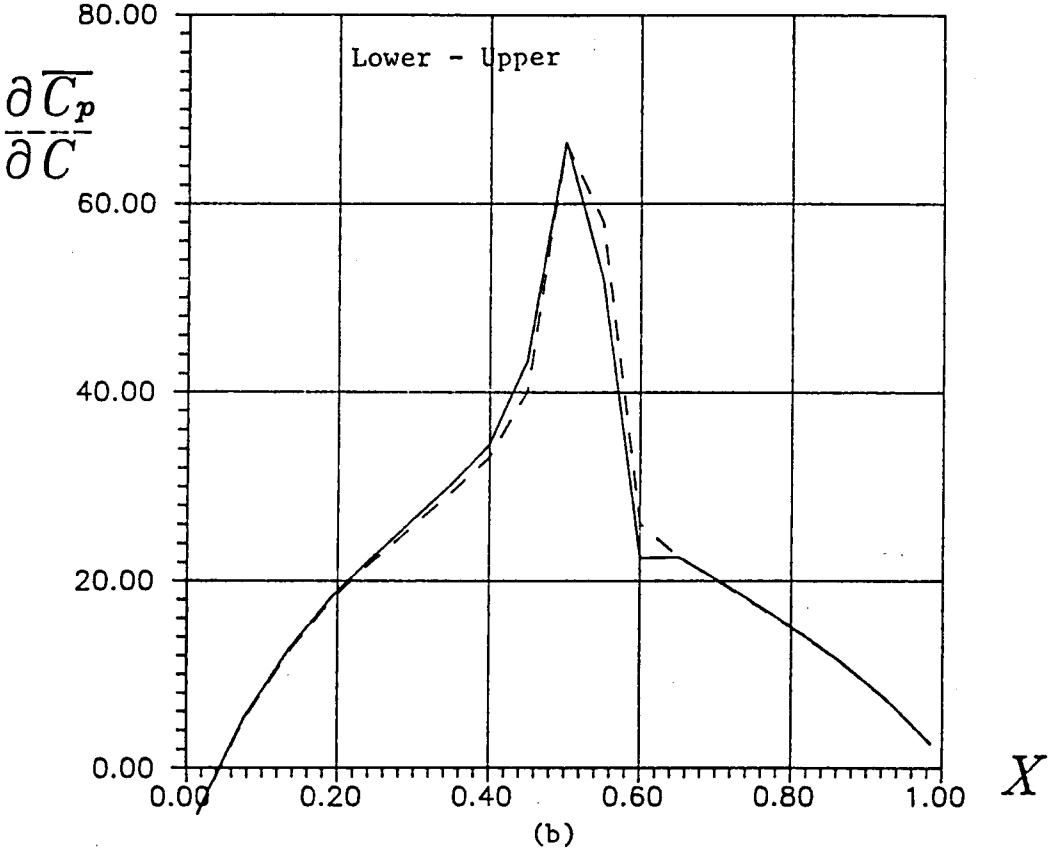

(b)

Figure 13 -- Sensitivity of Pressure to Maximum Camber
P1406 Airfoil M = 0.8 α = 1 degree

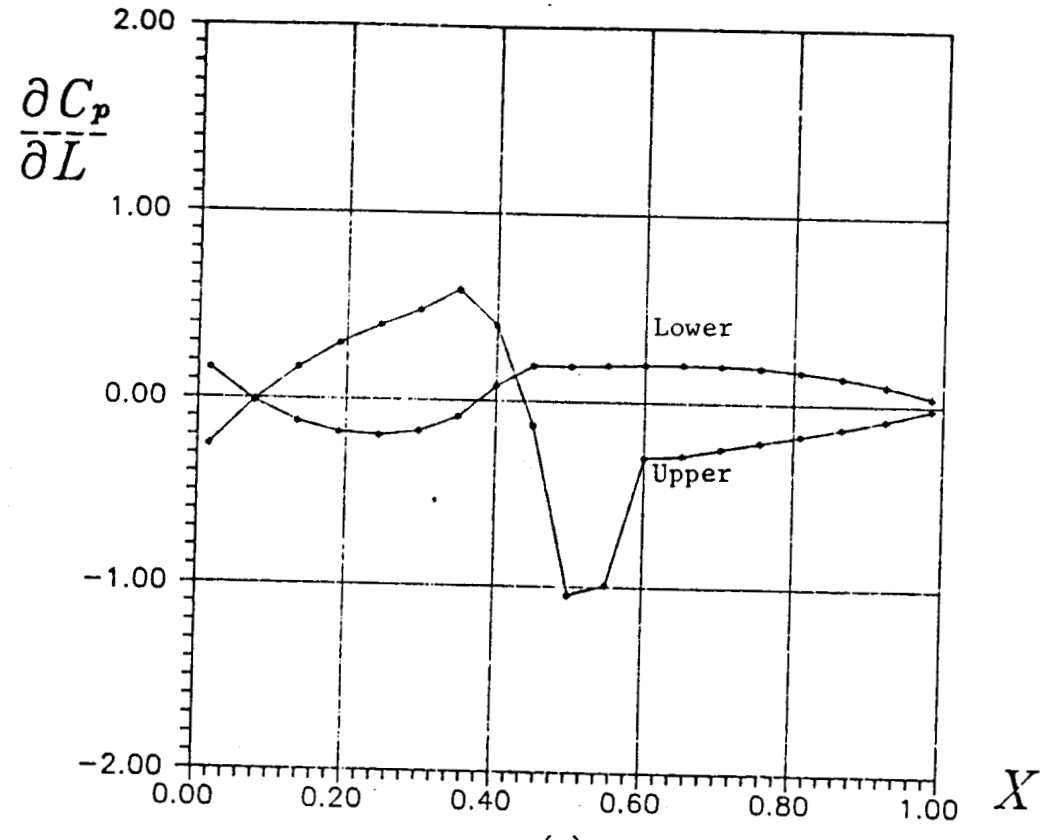

(a)

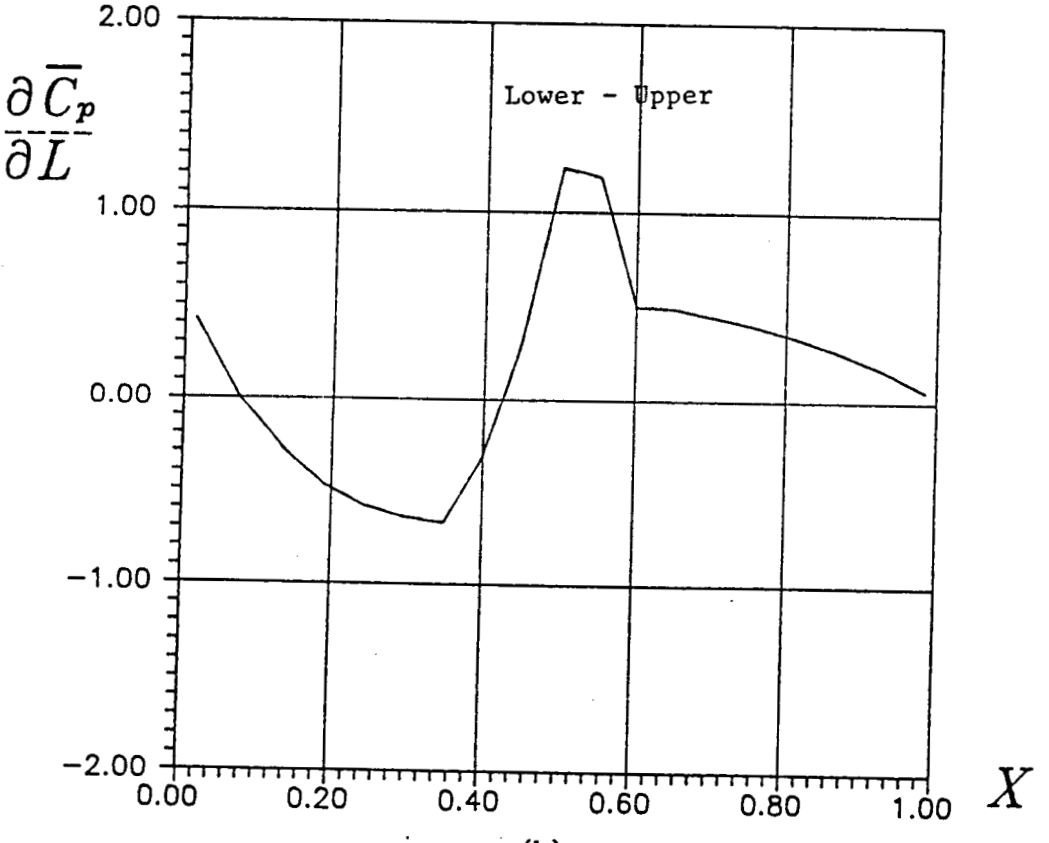

(b)

Figure 14 -- Sensitivity of Pressure to Location of Maximum Camber
P1406 Airfoil M = 0.8 α=1 degree

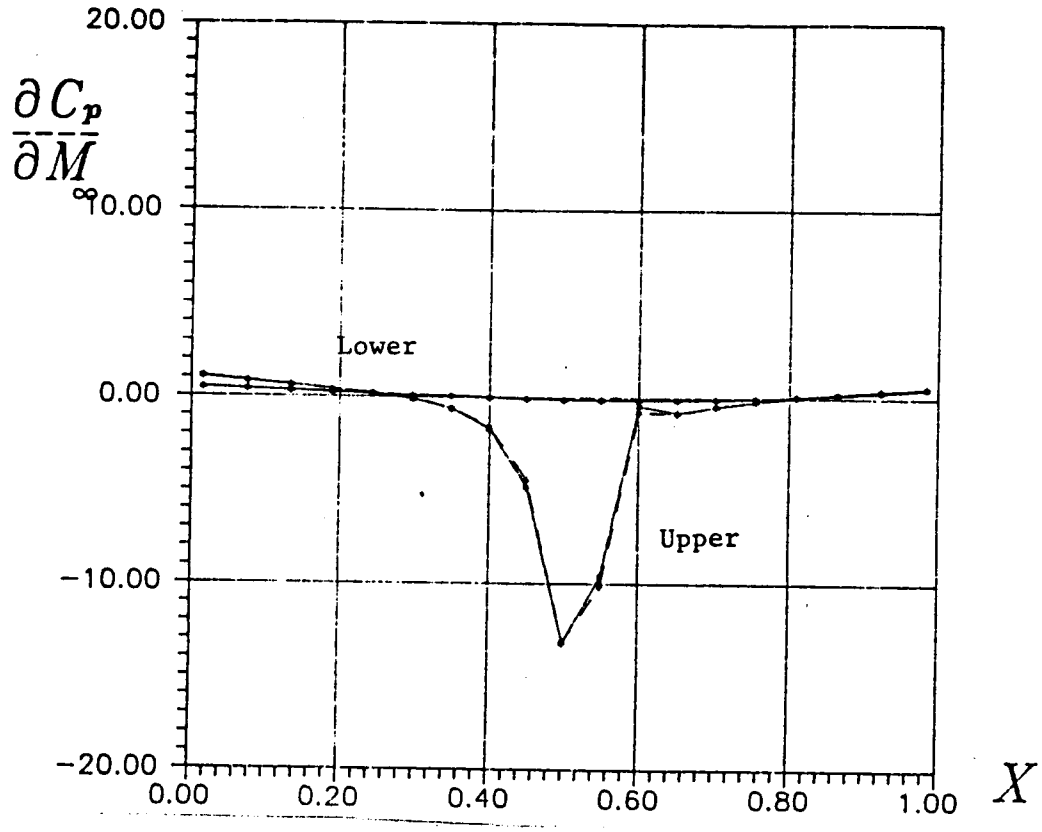

(a)

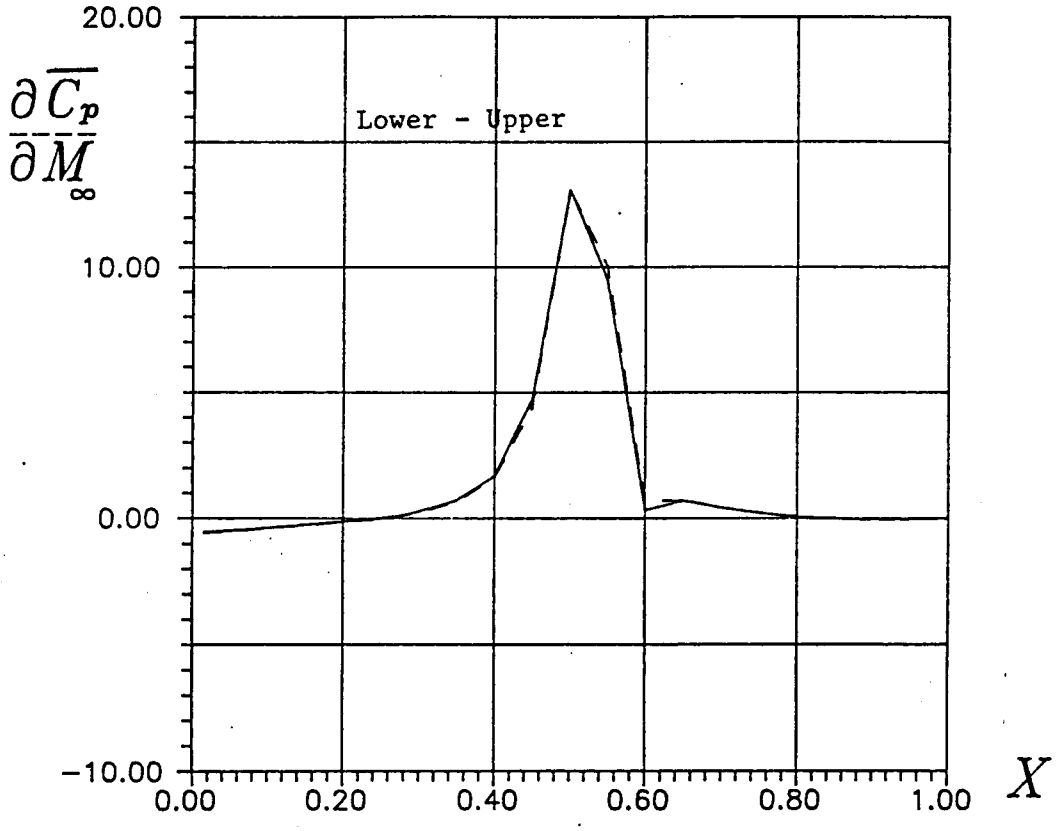

(b)

Figure 15 -- Sensitivity of Pressure to Mach Number
P1406 Airfoil M = 0.8 α = 1 degree

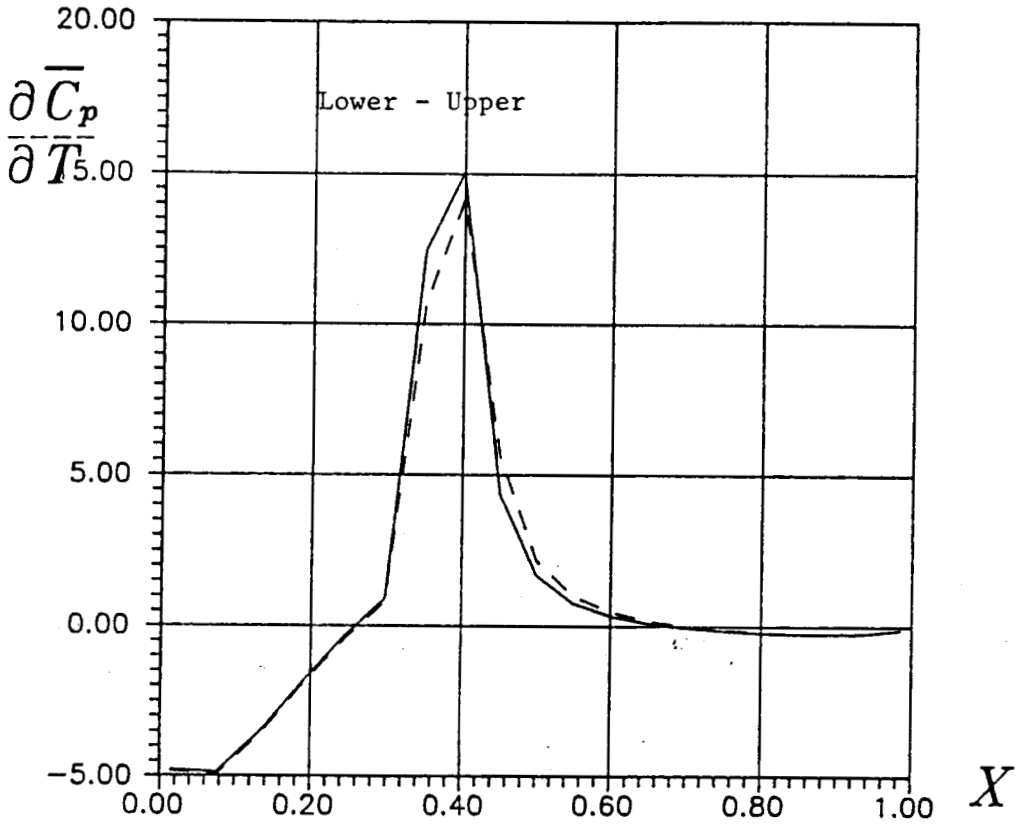

Figure 16 -- Sensitivity of Pressure to Maximum Thickness
NACA 1406 Airfoil M = 0.8 α = 1 degree

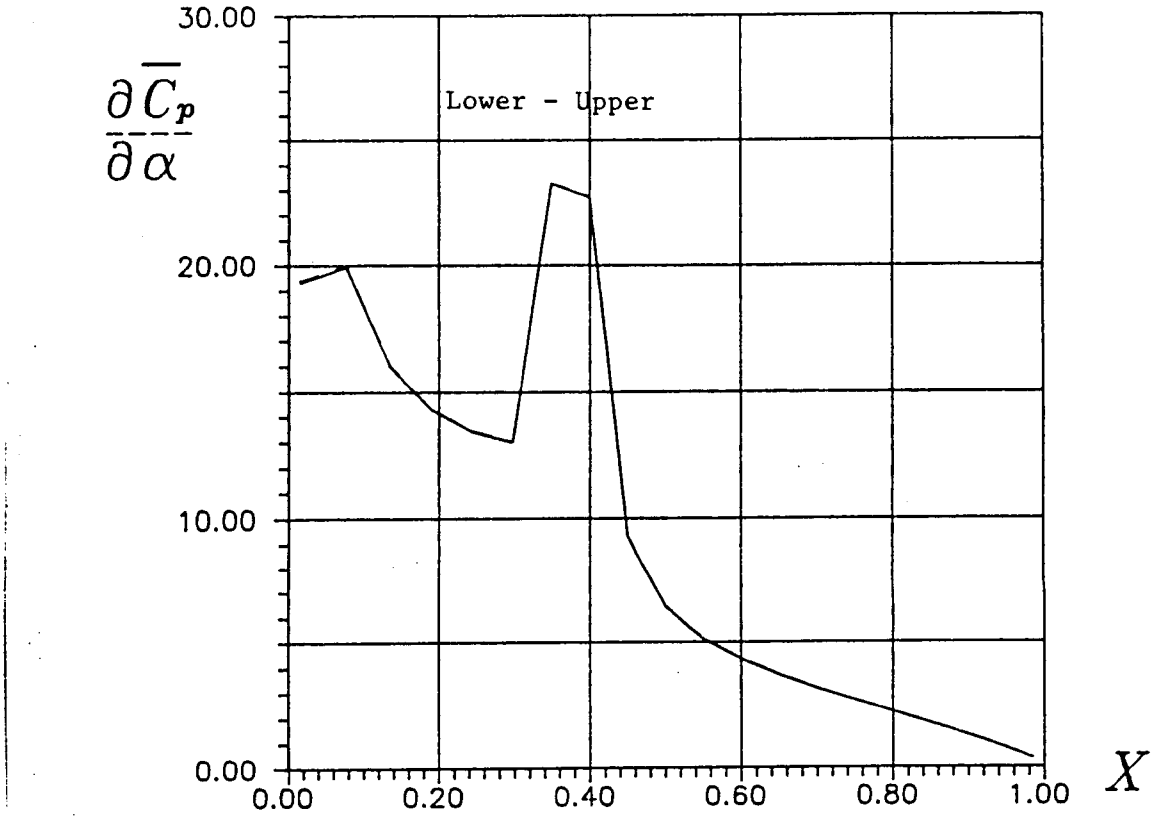

Figure 17 -- Sensitivity of Pressure to Angle of Attack
NACA 1406 Airfoil M = 0.8 α = 1 degree

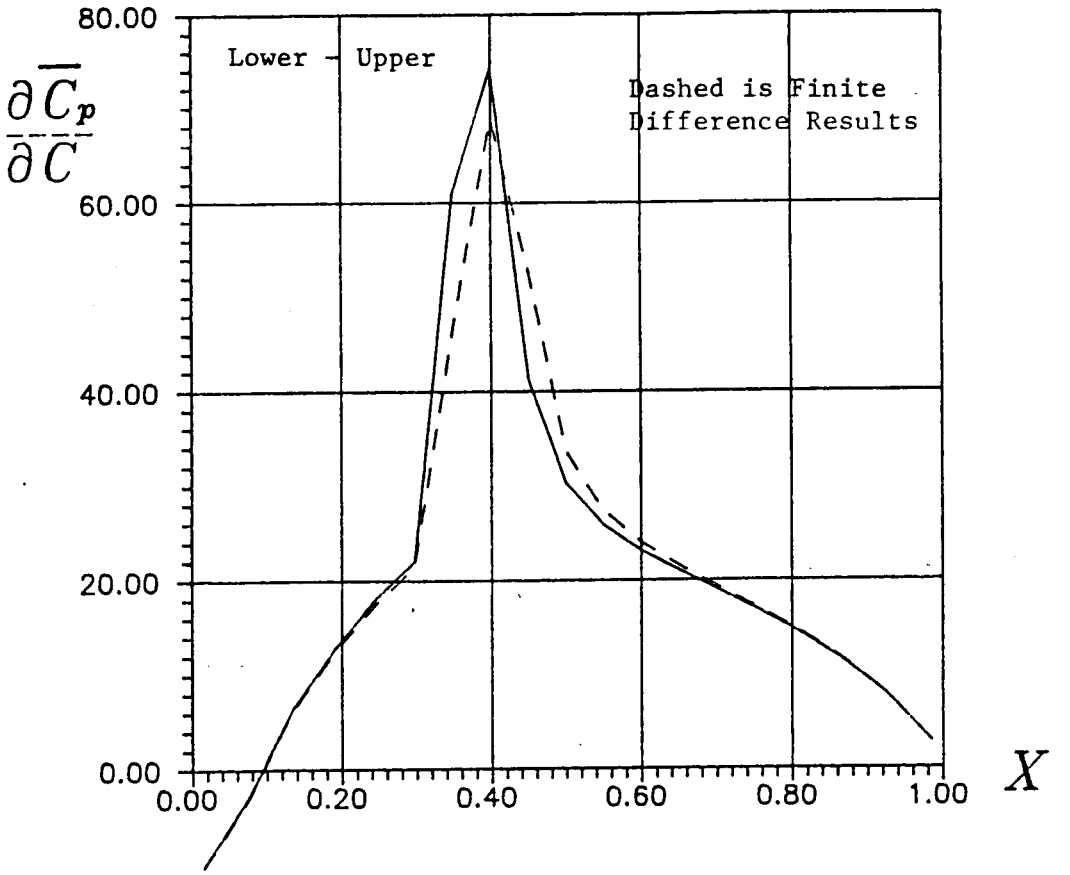

Figure 18 -- Sensitivity of Pressure to Maximum Camber
NACA 1406 Airfoil M = 0.8 α = 1 degree

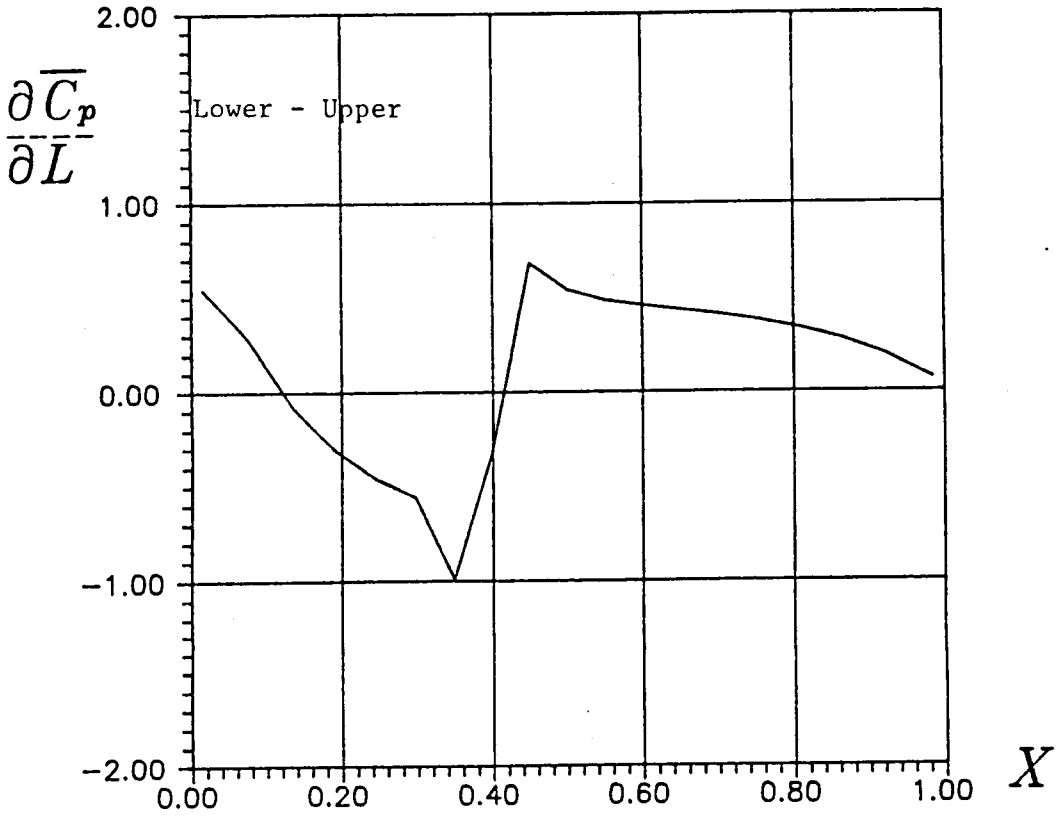

Figure 19 -- Sensitivity of Pressure to Location of Maximum Camber
NACA 1406 Airfoil M = 0.8 α = 1 degree

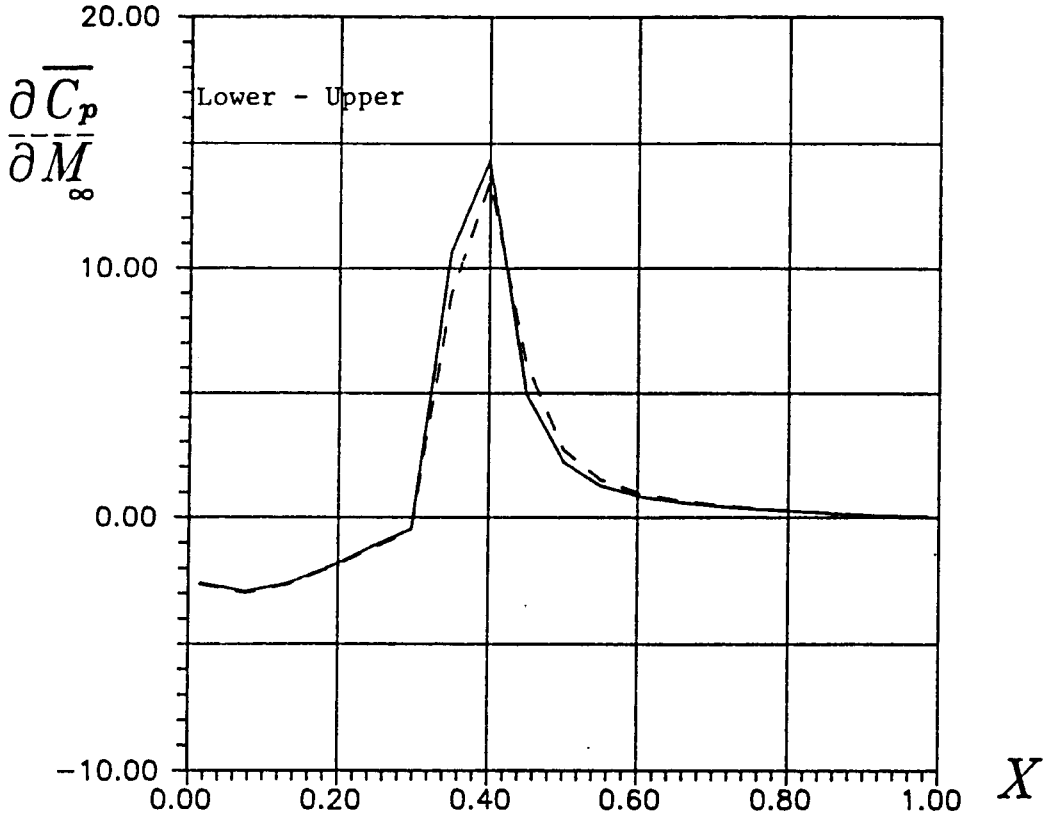

Figure 20 -- Sensitivity of Pressure to Mach Number
NACA 1406 Airfoil M = 0.8 α = 1 degree

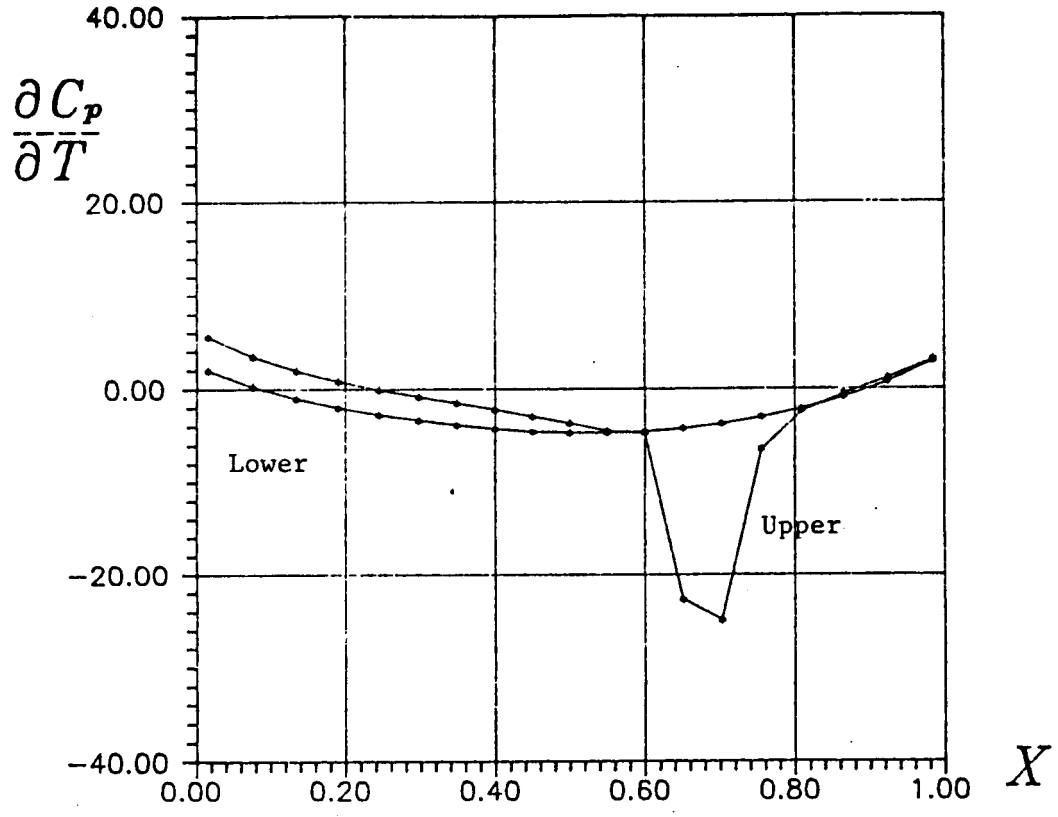

(a)

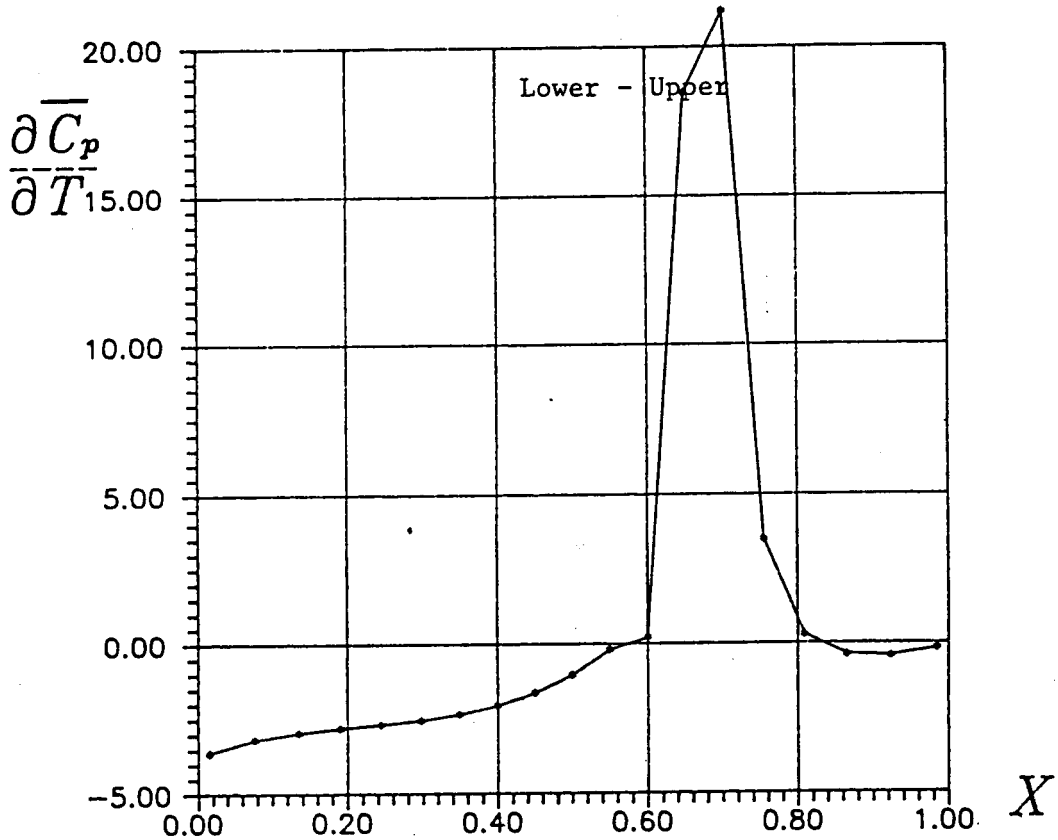

(b)

Figure 21 -- Sensitivity of Pressure to Maximum Thickness
P1406 Airfoil M = 0.825 $\breve{\alpha}$ = 1 degree

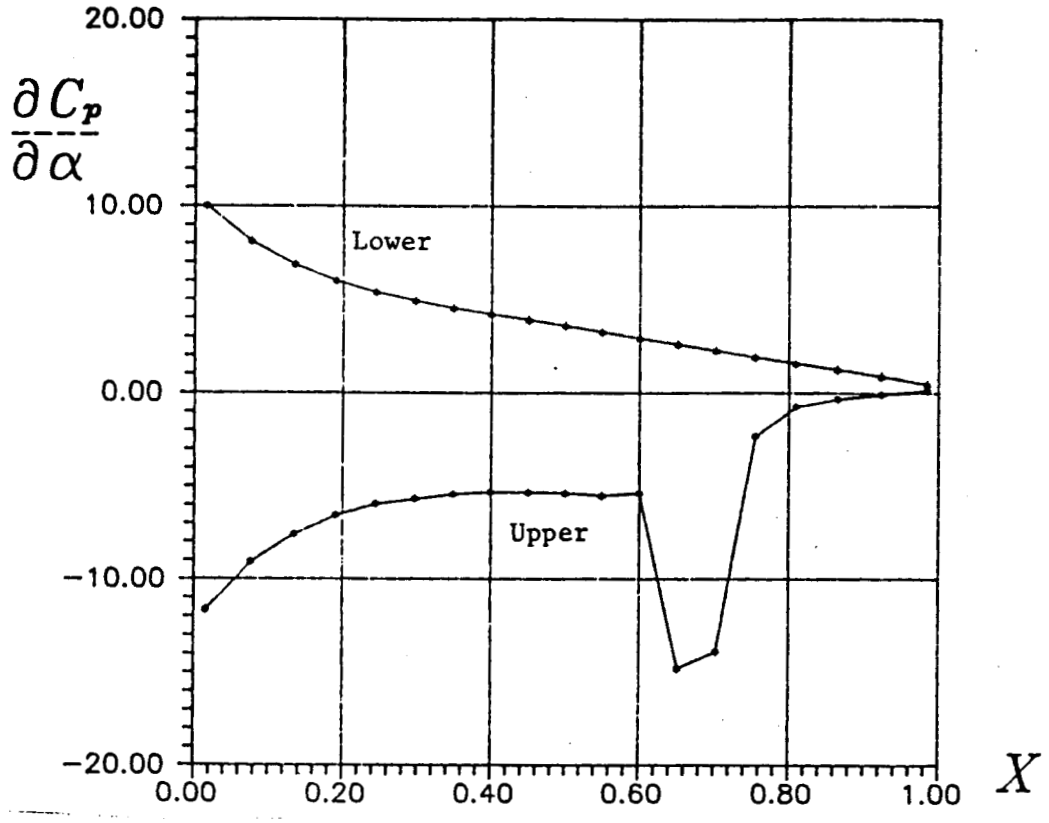

(a)

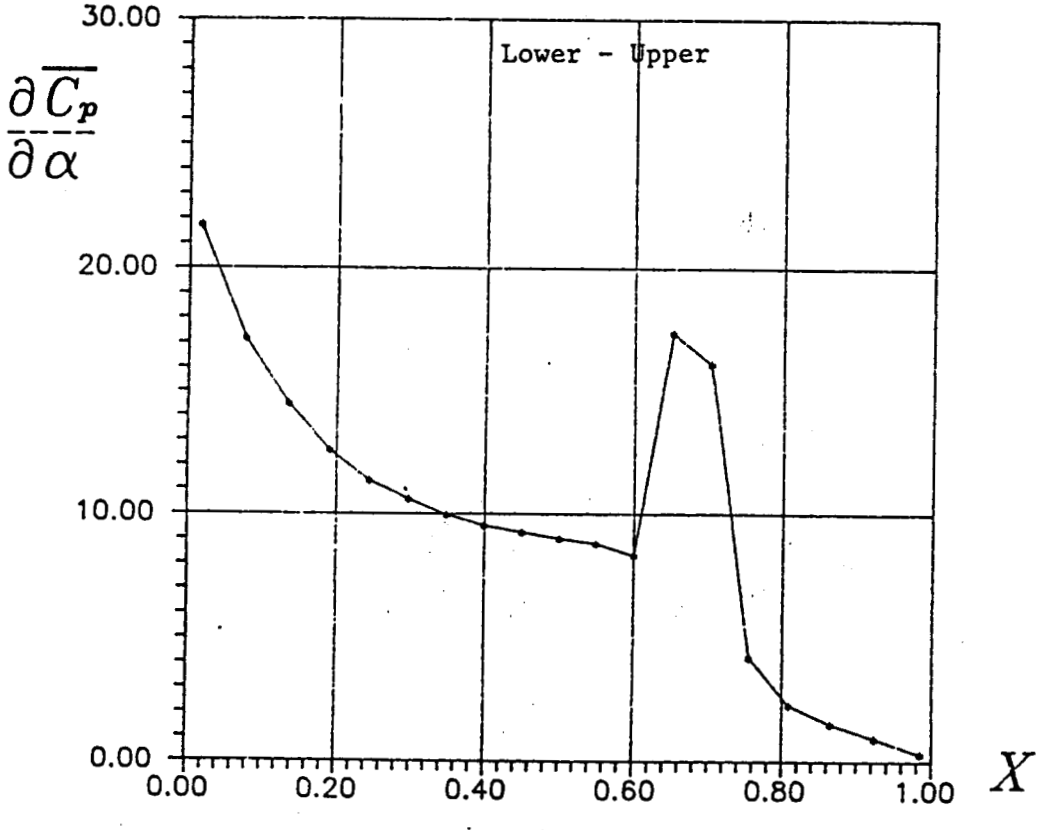

(b)

Figure 22 -- Sensitivity of Pressure to Angle of Attack
P1406 Airfoil M = 0.825 α = 1 degree

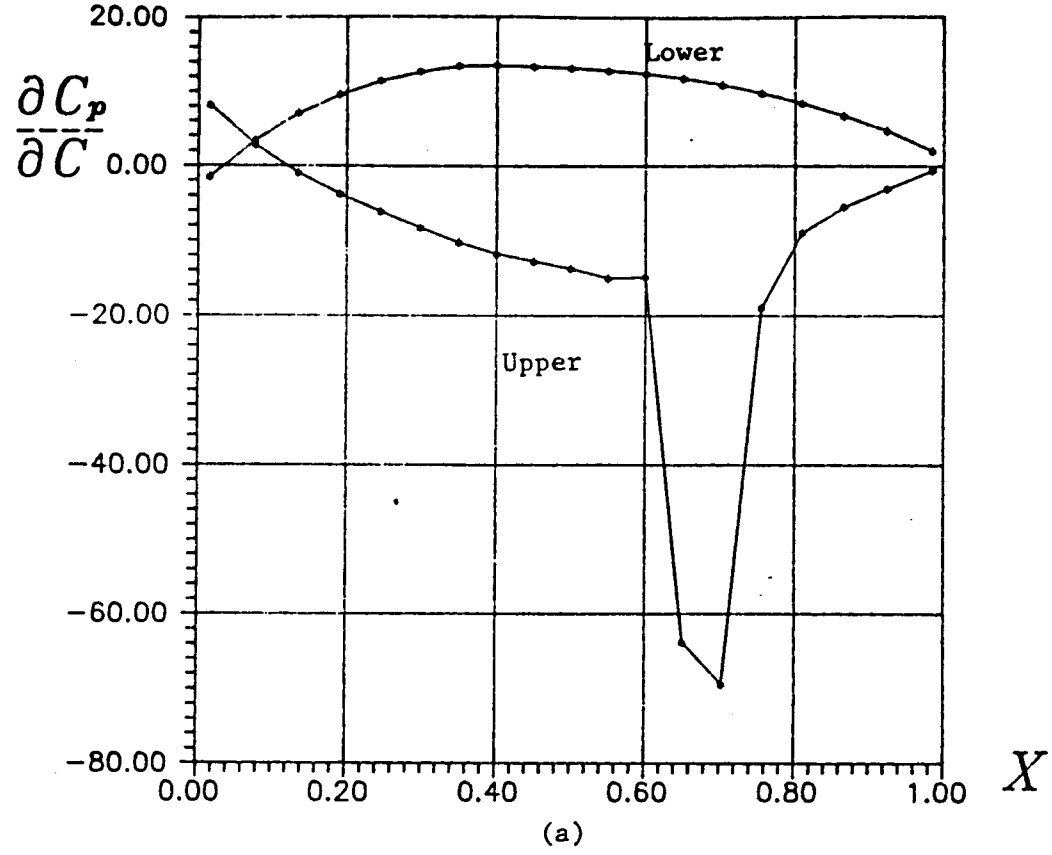

(a)

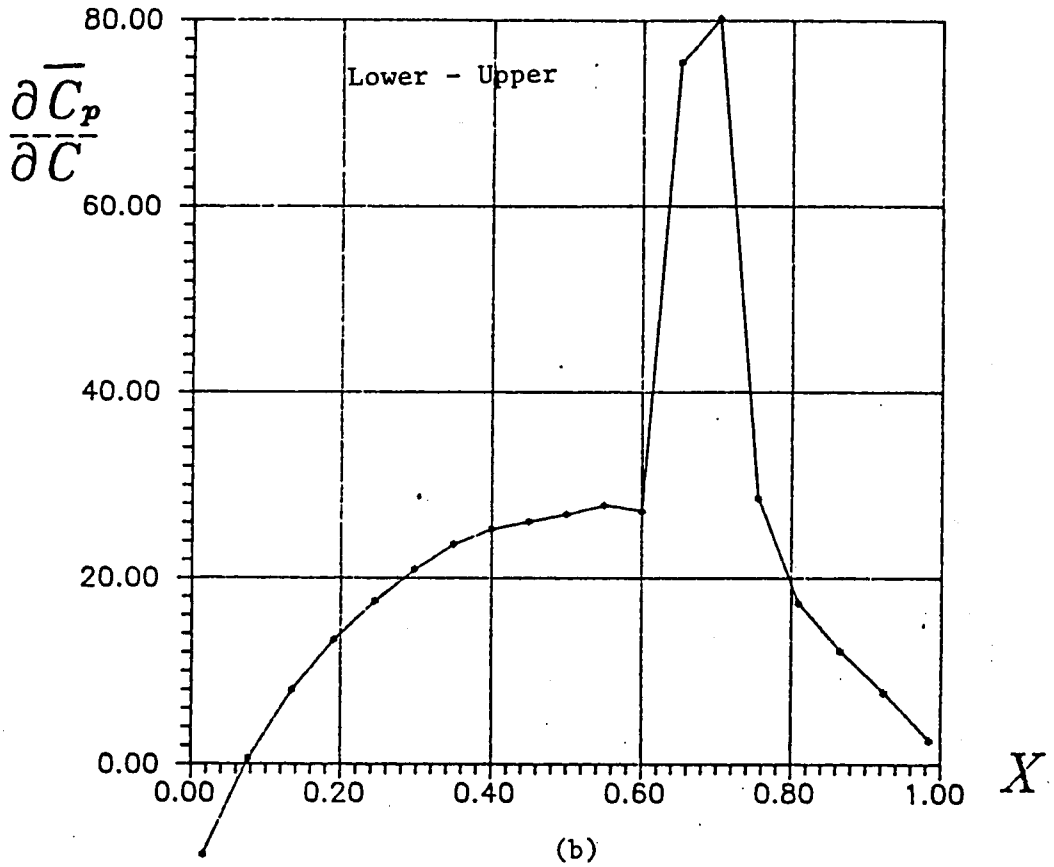

(b)

Figure 23 -- Sensitivity of Pressure to Maximum Camber
P1406 Airfoil M = 0.825 α = 1 degree

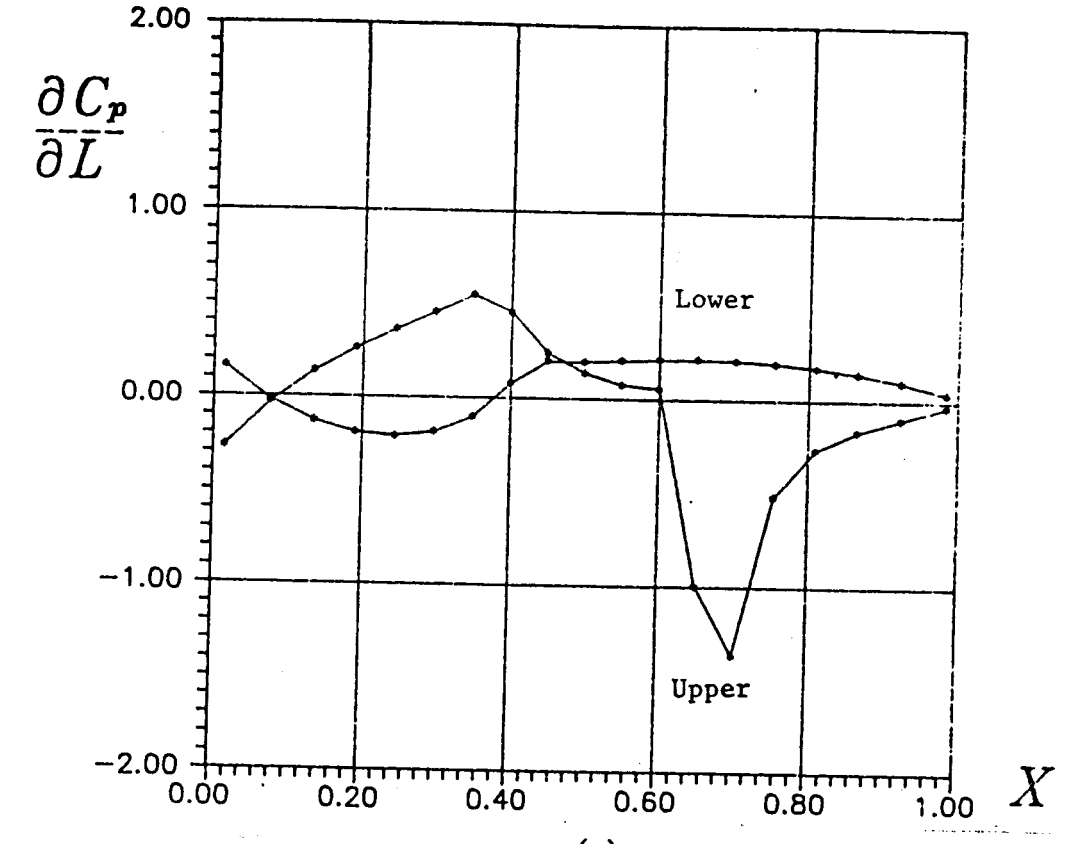

(a)

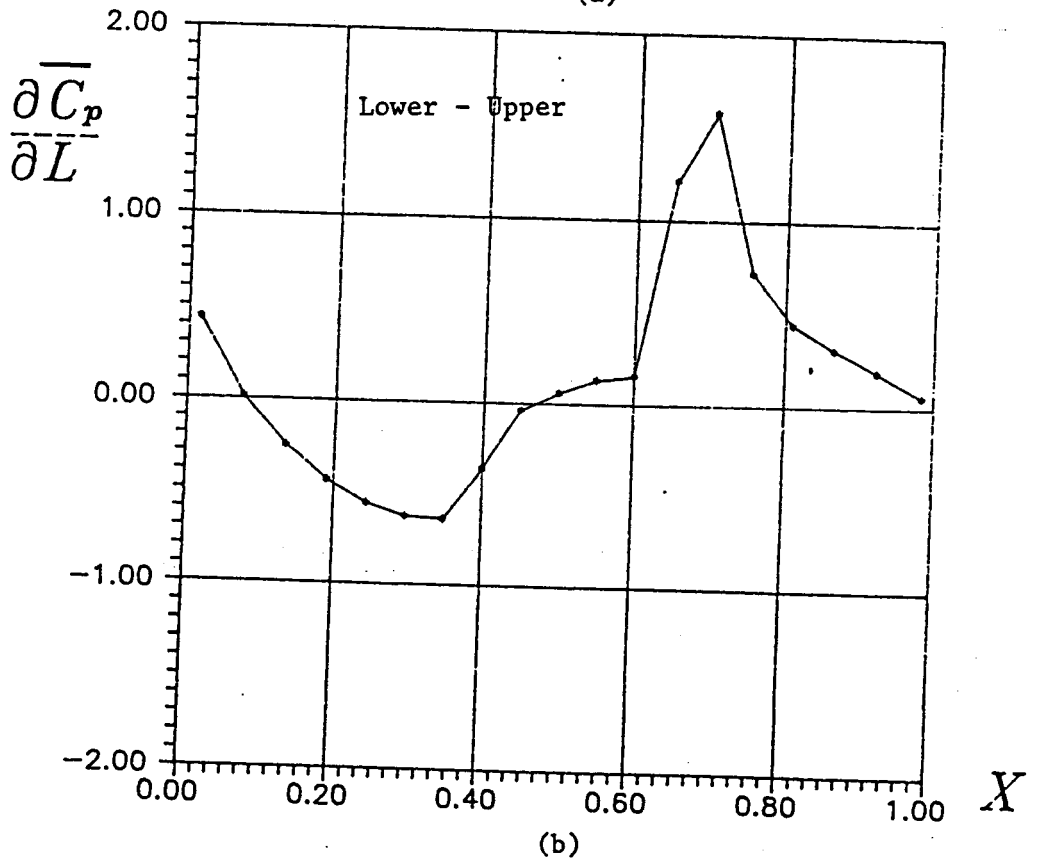

(b)

Figure 24 -- Sensitivity of Pressure to Location of Maximum Camber
P1406 Airfoil M = 0.825 α = 1 degree

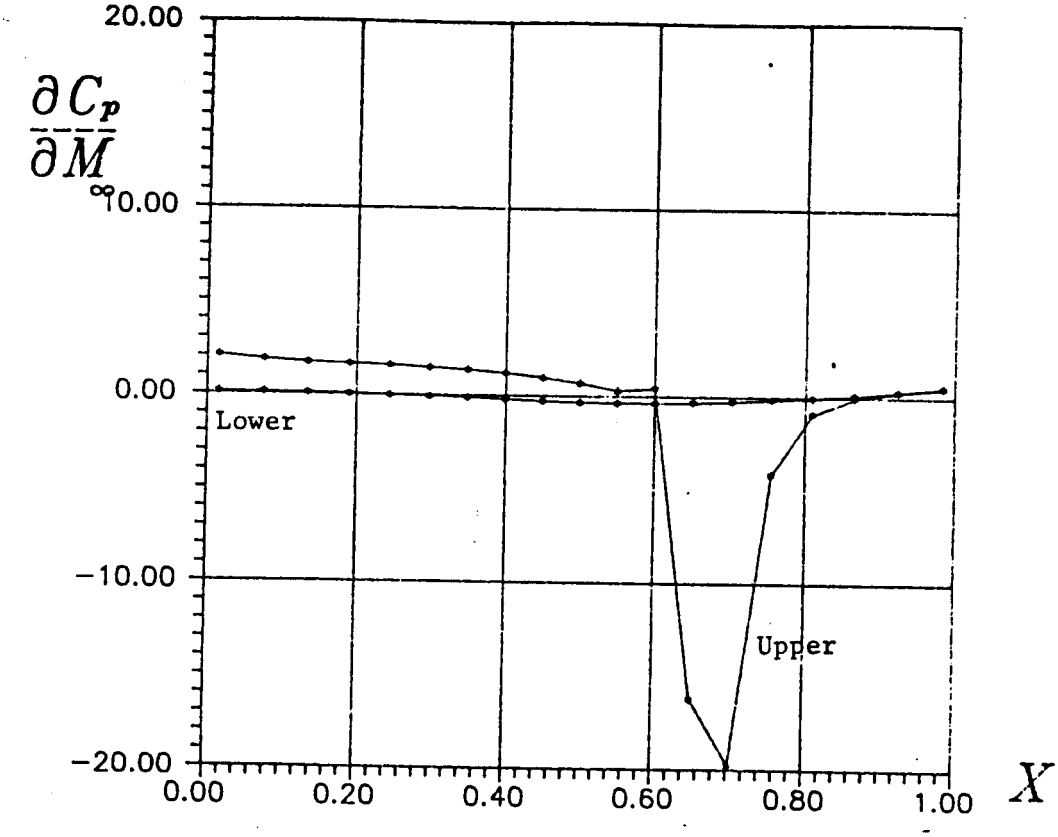

(a)

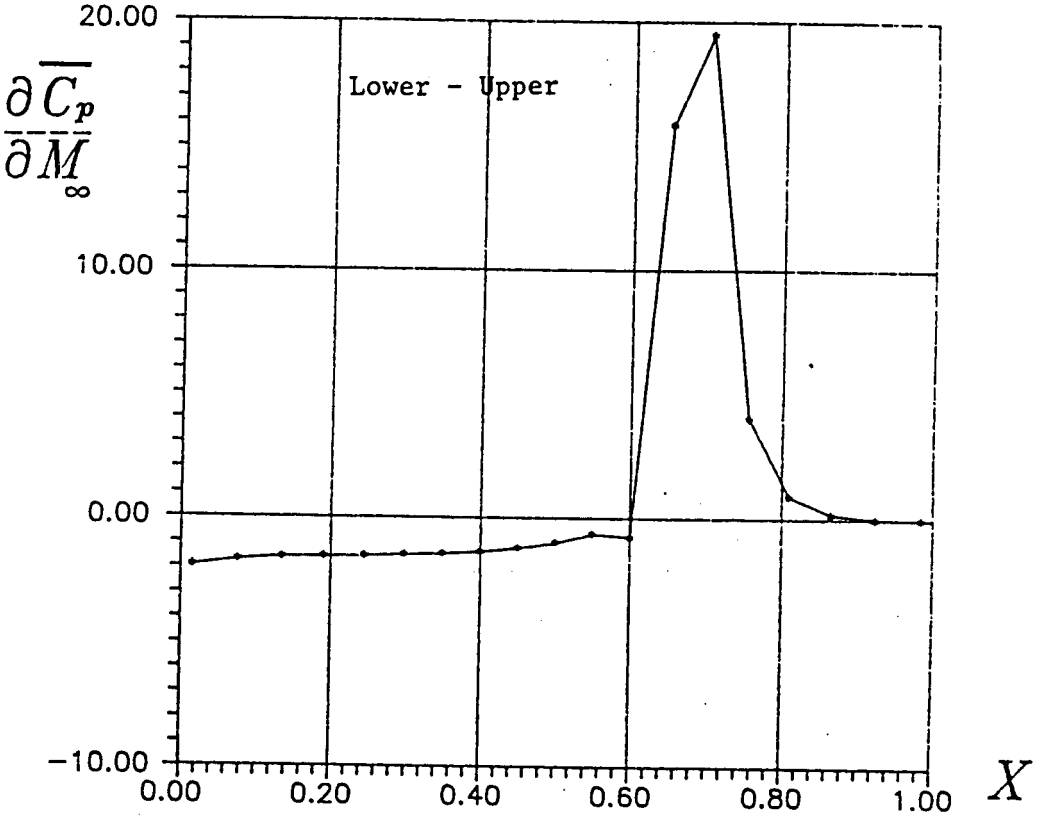

(b)

Figure 25 -- Sensitivity of Pressure to Mach Number
P1406 Airfoil M = 0.825 α = 1 degree

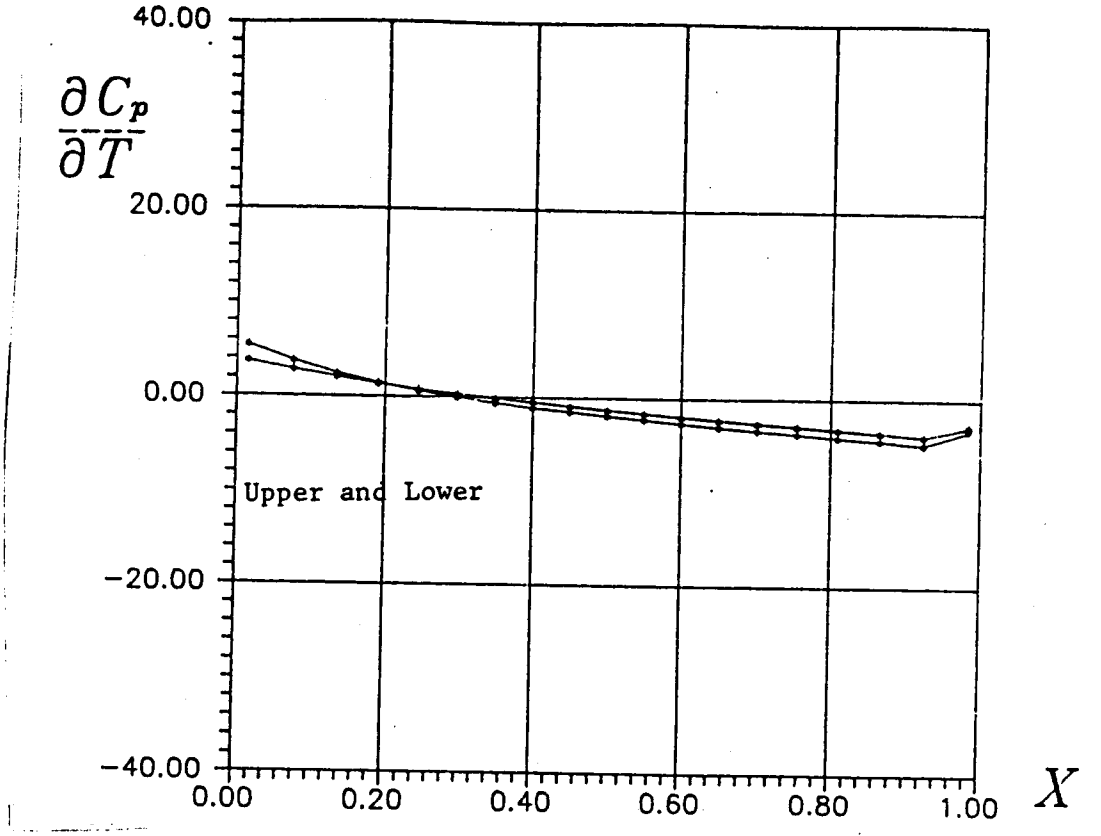

(a)

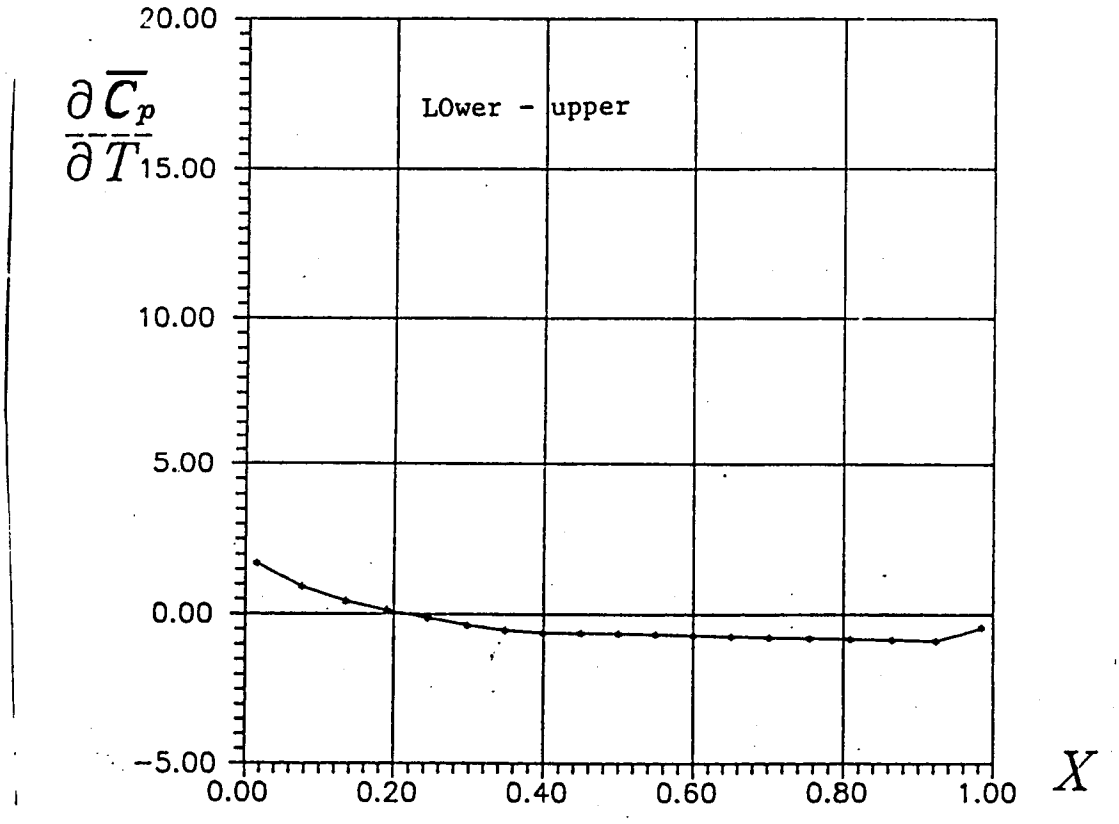

(b)

Figure 26 -- Sensitivity of Pressure to Maximum Thickness
P1406 Airfoil M = 1.2 α = 1 degree

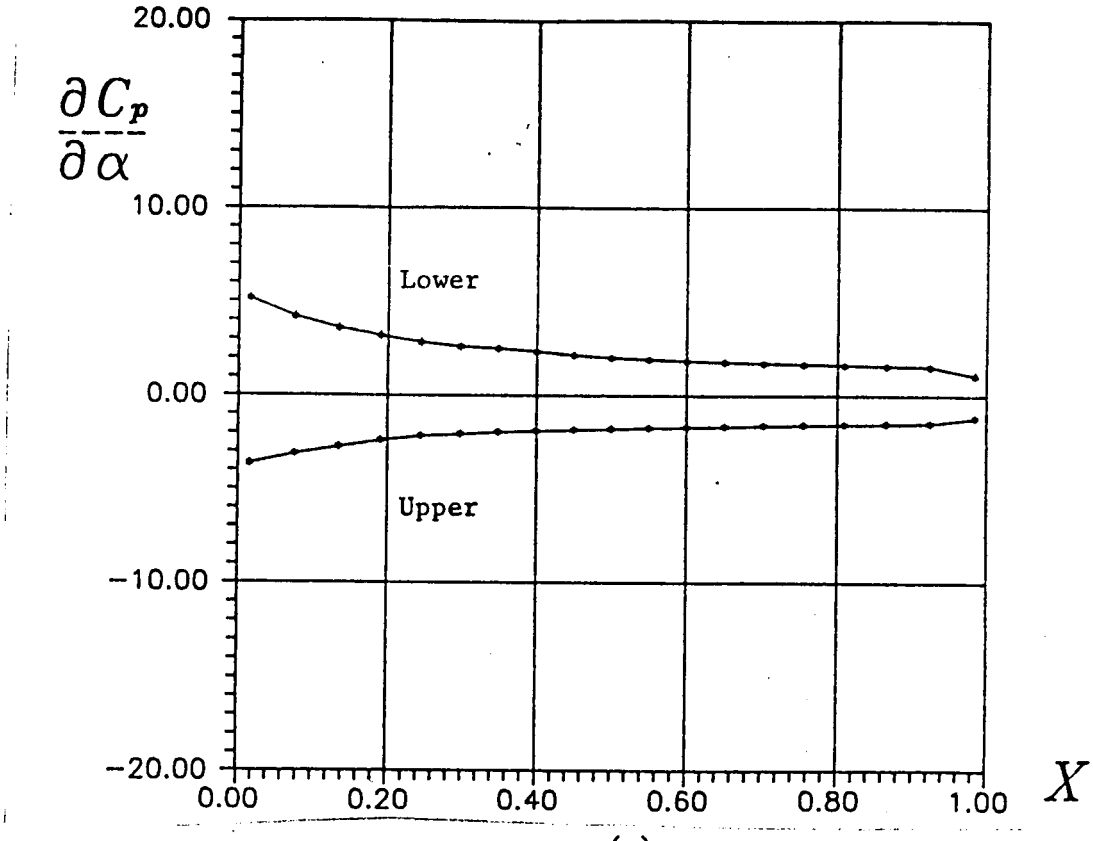

(a)

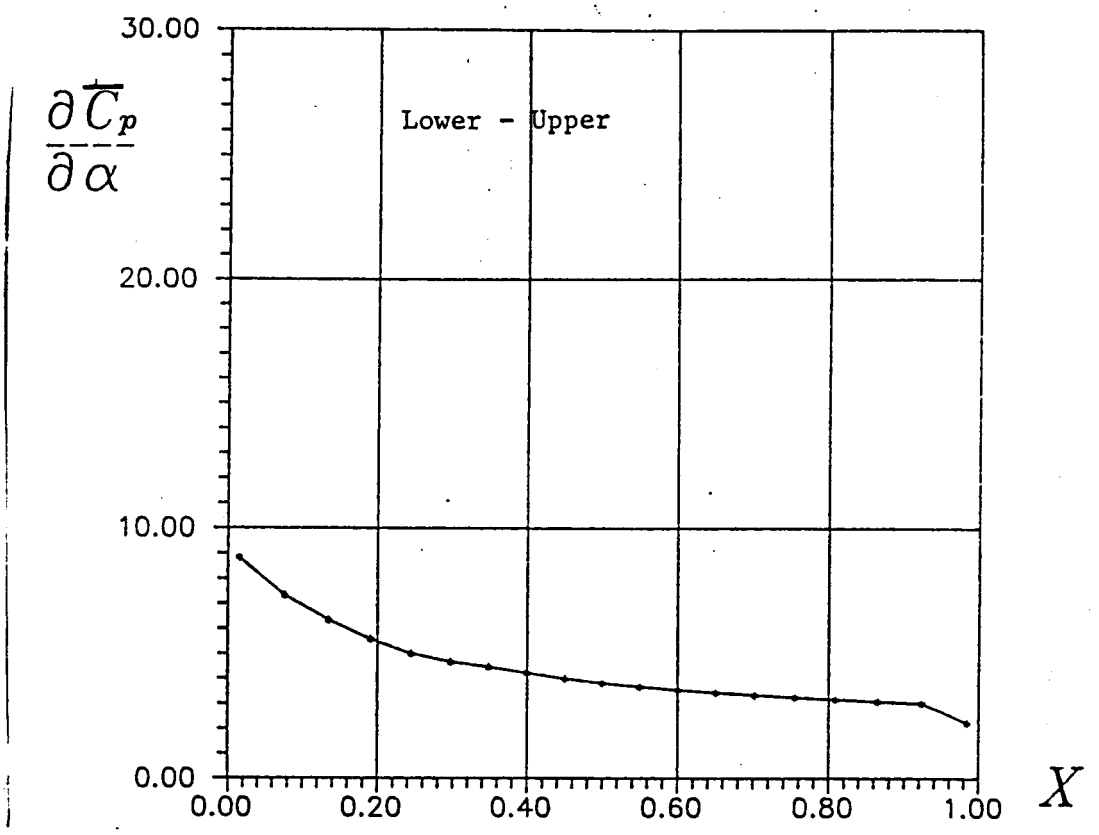

(b)

Figure 27 -- Sensitivity of Pressure to Angle of Attack
P1406 Airfoil M = 1.2 α,= 1 degree

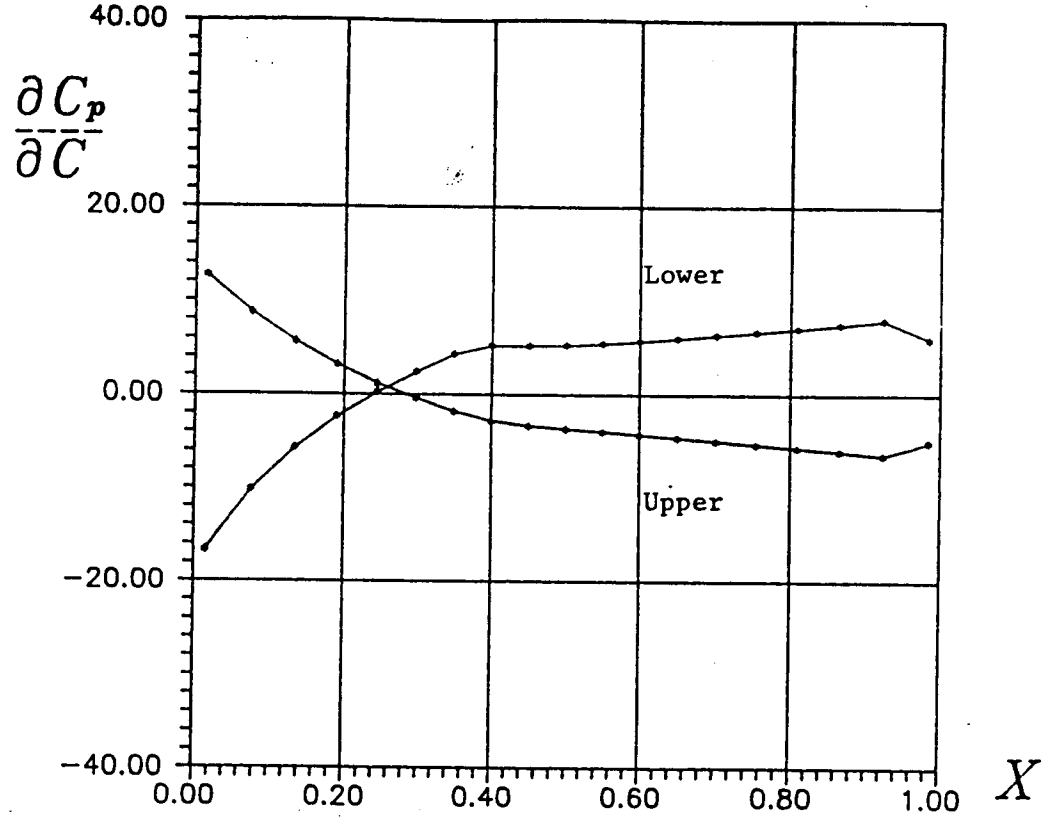

(a)

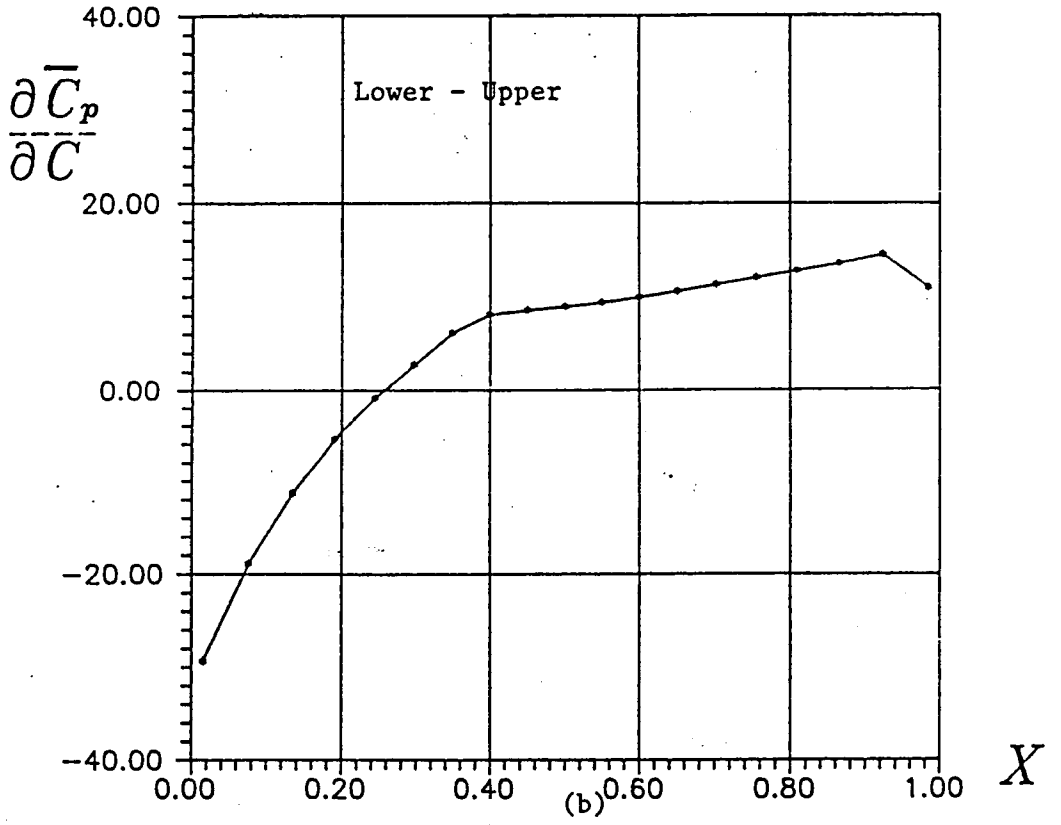

(b)

Figure 28 -- Sensitivity of Pressure to Maximum Camber
P1406 Airfoil M = 1.2 α = 1 degree

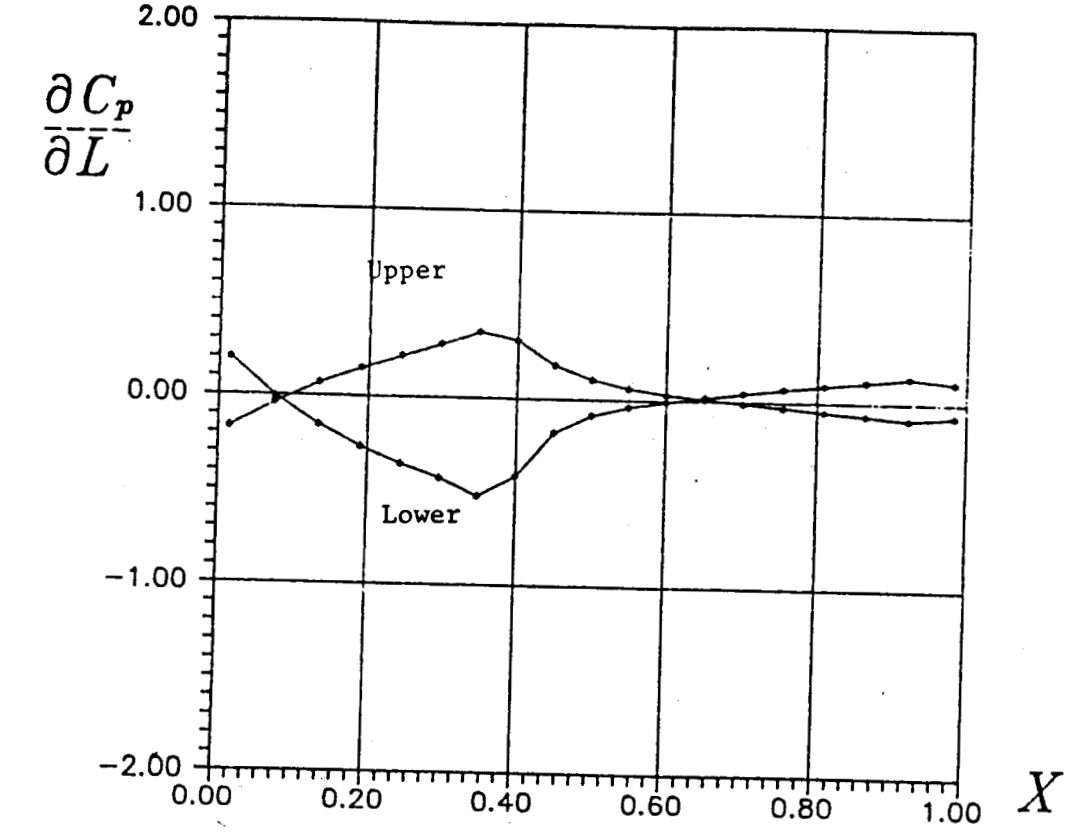

(a)

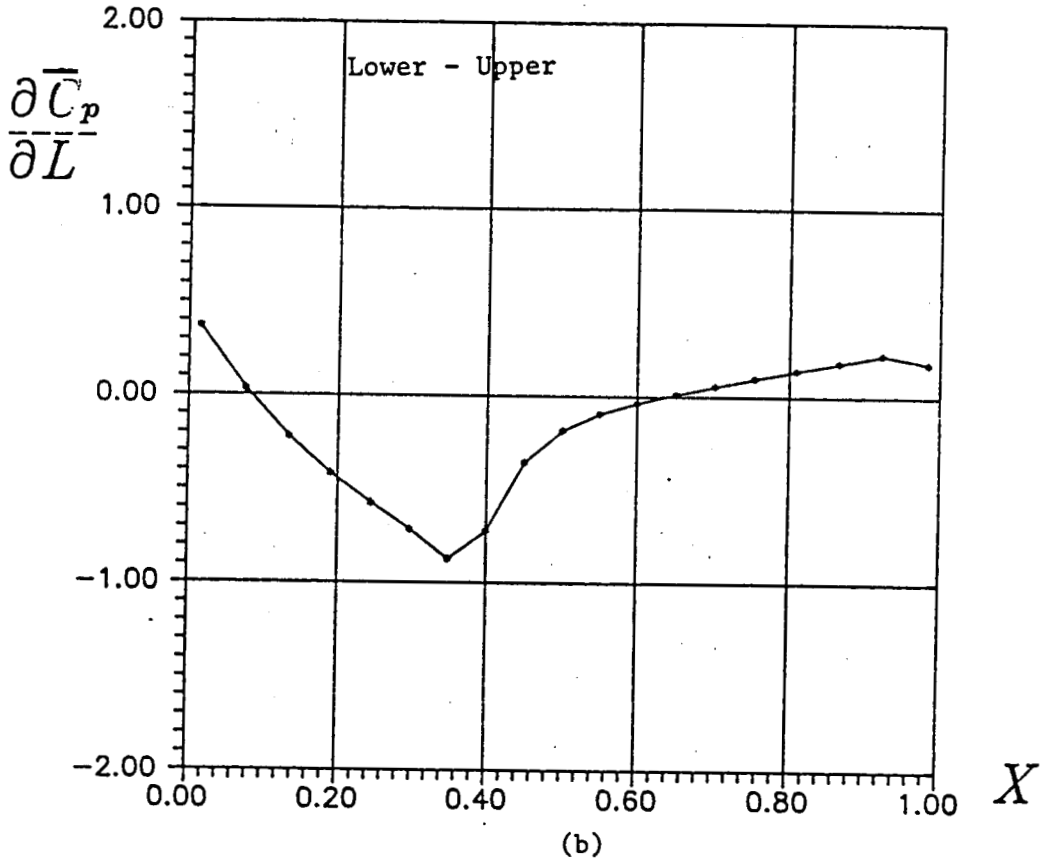

(b)

Figure 29 -- Sensitivity of Pressure to Location of Maximum Camber
P1406 Airfoil M = 1.2 α = 1 degree

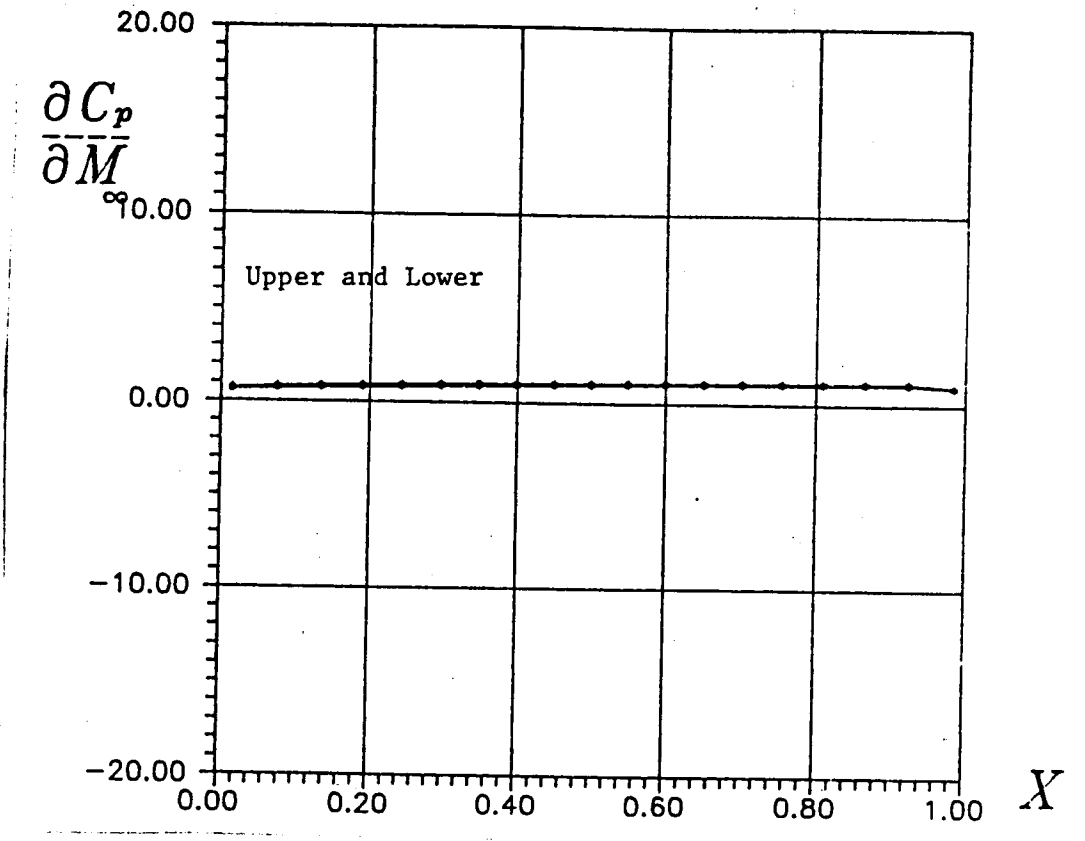

(a)

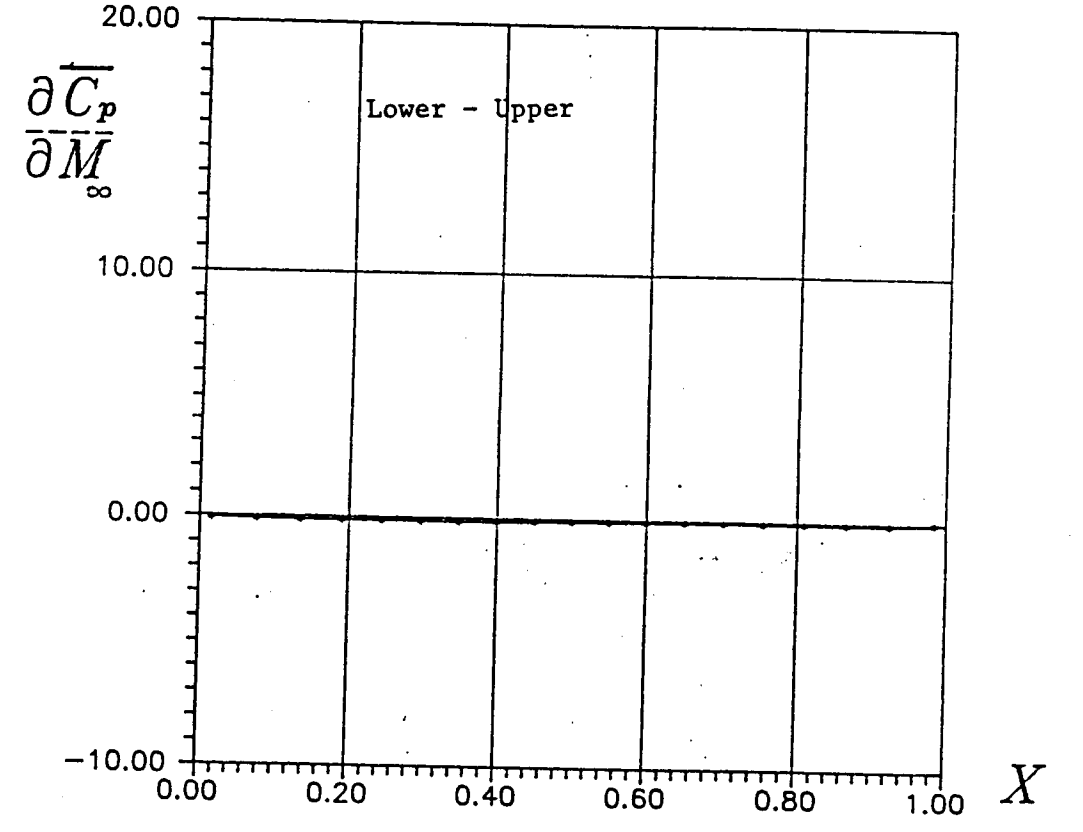

(b)

Figure 30 -- Sensitivity of Pressure to Mach Number
P1406 Airfoil M = 1.2 α = 1 degree